Eur. Phys. J. C 2, 373–392 (1998)

THE EUROPEAN PHYSICAL JOURNAL C


# Quantum effects on $t \longrightarrow H^+ b$ in the MSSM: a window to "virtual" supersymmetry?

J.A. Coarasa, David Garcia, Jaume Guasch, Ricardo A. Jiménez, Joan Solà

Grup de Física Teòrica, Institut de Física d'Altes Energies, Universitat Autònoma de Barcelona, E-08193 Bellaterra (Barcelona), Catalonia, Spain

Received: 18 April 1997 / Revised version: 18 June 1997

**Abstract.** We analyze the one-loop effects (strong and electroweak) on the unconventional top quark decay mode $t \to H^+ b$ within the MSSM. The results are presented in the on-shell renormalization scheme with a physically well motivated definition of $\tan\beta$. The study of this process at the quantum level is useful to unravel the potential supersymmetric nature of the charged Higgs emerging from that decay. As compared with the standard mode $t \to W^+ b$, the corrections to $t \to H^+ b$ are large, slowly decoupling and persist at a sizeable level even for all sparticle masses well above the LEP 200 discovery range. As a matter of fact, the potential size of the SUSY effects, which amount to corrections of several ten percent, could counterbalance the standard QCD corrections and even make them to appear with the "wrong" sign. Therefore, if the charged Higgs decay of the top quark is kinematically allowed – a possibility which is not excluded by the existing measurements of the branching ratio $BR(t \to W^+ b)$ at the Tevatron – it could be an invaluable laboratory to search for "virtual" supersymmetry. While a first significant test of these effects could possibly be performed at the upgraded Tevatron, a more precise verification would most likely be carried out in future experiments at the LHC.

## 1 Introduction

Recently, the Standard Model (SM) of the strong and electroweak interactions has been crowned with the discovery of the penultimate building block of its theoretical structure: the top quark, $t$ [1]. At present the best determination of the top-quark mass at the Tevatron reads as follows [2]:

$$m_t = 175 \pm 6\ GeV\,. \tag{1}$$

While the SM has been a most successful framework to describe the phenomenology of the strong and electroweak interactions for the last thirty years, the top quark itself stood, at a purely theoretical level – namely, on the grounds of requiring internal consistency, such as gauge invariance and renormalizability – as a firm prediction of the SM since the very confirmation of the existence of the bottom quark and the measurement of its weak isospin quantum numbers [3]. With the finding of the top quark, the matter content of the SM has been fully accounted for by experiment. Still, the last building block of the SM, viz. the fundamental Higgs scalar, has not been found yet, which means that in spite of the great significance of the top quark discovery the theoretical mechanism by which all particles acquire their masses in the SM remains experimentally unconfirmed. Thus, it is not clear at present whether the SM will remain as the last word in the phenomenology of the strong and electroweak interactions around the Fermi's scale or whether it will be eventually subsumed within a larger and more fundamental theory. The search for physics beyond the SM, therefore, far from been accomplished, must continue with redoubled efforts. Fortunately, the peculiar nature of the top quark (in particular its large mass – in fact, perhaps the heaviest particle in the SM! – and its characteristic interactions with the scalar particles) may help decisively to unearth any vestige of physics beyond the SM.

In this paper, we shall focus our attention on hypothetical top quark physics associated to the (minimal) SUSY extension of the SM, the MSSM [4], which is at present the most predictive framework for physics beyond the SM and, in contradistinction to all other approaches, it has the virtue of being a fully-fledged Quantum Field Theory. Most important, on the experimental side the global fit analyses to all indirect precision data within the MSSM are comparable to those in the SM; in particular, the MSSM analysis implies that $m_t = 172 \pm 5\, GeV$ [5], a result which is compatible with the above mentioned experimental determinations of $m_t$. Hints of this new phenomenology may show up either in the form of direct or virtual effects from supersymmetric Higgs particles or from the "sparticles" themselves (i.e. the $R$-odd [4] partners of the SM particles), in particular from the top-squark ("stop") which is the SUSY counterpart of the top quark. Due to the huge mass of the latter, one expects that the top-stop system is one of the most preferential chiral supermultiplets to which the Higgs sector should couple. Therefore, top quark dynamics is deemed to be an ideal environment

for Higgs phenomenology and a most suitable SUSY trigger, if SUSY is there at all.

In the MSSM the spectrum of Higgs-like particles and of Yukawa couplings is far and away richer than in the SM. In this respect, a crucial fact affecting the results of our work is that in such a framework the bottom-quark Yukawa coupling may counterbalance the smallness of the bottom mass, $m_b \simeq 5\,GeV$, at the expense of a large value of $\tan\beta$ – the ratio of the vacuum expectation values (VEV's) of the two Higgs doublets – the upshot being that the top-quark and bottom-quark Yukawa couplings (normalized with respect to the $SU(2)$ gauge coupling) as they stand in the superpotential, take on the form

$$\lambda_t \equiv \frac{h_t}{g} = \frac{m_t}{\sqrt{2}\, M_W\, \sin\beta}, \lambda_b \equiv \frac{h_b}{g} = \frac{m_b}{\sqrt{2}\, M_W\, \cos\beta}\,. \quad (2)$$

Thus, depending on the actual value of $\tan\beta$, $\lambda_b$ and $\lambda_t$ can be of the same order of magnitude, perhaps even showing up in "inverse hierarchy": $\lambda_b > \lambda_t$ for $\tan\beta > m_t/m_b$. Notice that due to the perturbative bound $\tan\beta \lesssim 70$ one never reaches a situation where $\lambda_t << \lambda_b$. In a sense, $\lambda_b \simeq \lambda_t$ could be judged as a natural relation in the MSSM; it can even be a necessary relation in specific SUSY-GUT models, e.g. those based on $t, b$ and $\tau$ Yukawa coupling unification [6], at least at the unification point. Furthermore, one expects that if such a relation holds, then it is not just the top-stop system, but also the bottom-sbottom chiral supermultiplet that could play a momentous role in the quantum physics of the top and bottom quarks. Indeed, since the Higgs sector of the MSSM doubles that of the SM, and it comes associated with the fermionic SUSY partners – the so-called higgsinos –, one expects that in the limit $\lambda_b \gtrsim \lambda_t$ there should occur a very stimulating dynamics triggered by the presence of a rich variety of potentially large Yukawa-like interactions formed out of the top/stop-bottom/sbottom-Higgs/higgsino fields.

A particularly brilliant form of this dynamics, on which we shall focus our attention, is revealed through the study of the quantum effects on the non-standard top quark decay into a charged Higgs: $t \to H^+ b$. This decay, which has already deserved some attention in the early literature on the subject [7], is not at all excluded by the recent measurements (at the Tevatron) of the branching ratio of the standard top quark decay, $t \to W^+ b$, as will be discussed in more detail in Sect. 2. The quantum effects on $t \to H^+ b$, which we wish to compute in the framework of the MSSM at one-loop, can be both strong and electroweak like. Of these the conventional strong corrections (QCD) mediated by gluons have already been treated in detail [8]. Also the subset of strong supersymmetric corrections mediated by gluinos, stop and sbottom squarks, i.e. the SUSY-QCD corrections, has been discussed in [9]. Here, therefore, we will come to grips with the remaining part – as a mater of fact, the largest and most difficult part – of the MSSM corrections: namely, the multifarious electroweak supersymmetric corrections produced by squarks, sleptons, charginos, neutralinos and supersymmetric Higgs bosons, which we shall combine with the total strong (QCD +SUSY-QCD) corrections to obtain the MSSM correction.

In the present study, we will closely follow the systematic pathway adopted in the treatment of the MSSM quantum corrections to the canonical decay $t \to W^+ b$ [10]–[12]. However, because of the Higgs particle in the final state, we have to incorporate the details of the renormalization of the Higgs sector of the MSSM, which substantially alter the analytical counterterm structure of the $t\,b\,H^+$-vertex as compared to the conventional $t\,b\,W^+$-vertex. In this paper we take the point of view that the study of the decay $t \to H^+ b$ is worthwhile provided that its branching ratio is operative at a level $BR(t \to H^+ b) > 10\%$, a condition which is not ruled out by the top quark experiments. Theoretically, this is fully guaranteed provided that $\tan\beta$ is large enough ($\gtrsim 30$). In these conditions, the MSSM one-loop corrections can typically be in the 50% ballpark.

The paper is organized as follows. In Sect. 2 the lowest order relations concerning the Higgs sector and the top quark decay are given. We also discuss the status of the charged Higgs decay of the top quark in the light of the recent data from Tevatron, and the prospects for its detection. Section 3 discusses the renormalization of the $t\,b\,H^+$-vertex in the on-shell scheme with a physically well motivated definition of $\tan\beta$. In Sect. 4 we present the full analytical formulae for the one-loop corrected partial width $\Gamma(t \to H^+ b)$ in the MSSM. The numerical analysis and discussion, as well as the conclusions, are delivered in Sect. 5.

## 2 Lowest order relations and determination of $BR(t \to H^+ b)$ from experiment

In this paper we wish to emphasize the possibility that a charged pseudoscalar, $H^\pm$, involved in a possible unconventional decay of the top-quark, $t \to H^+ b$, be the charged Higgs of the MSSM [1]. A charged Higgs is necessary in the MSSM since Supersymmetry requires the existence of at least two Higgs $SU(2)_L$-doublets with opposite weak-hypercharges to give masses to matter and gauge fields:

$$H_1 = \begin{pmatrix} H_1^0 \\ H_1^- \end{pmatrix} \quad (Y=-1)\,, \qquad H_2 = \begin{pmatrix} H_2^+ \\ H_2^0 \end{pmatrix} \quad (Y=+1)\,. \quad (3)$$

Because of the SUSY constraints, the structure of the Higgs potential of the MSSM constructed out of the two doublets (3) takes on the form [14]:

$$V = m_1^2\,|H_1|^2 + m_2^2\,|H_2|^2 - m_{12}^2\,\left(\epsilon_{ij}\,H_1^i\,H_2^j + \text{h.c.}\right) + \frac{1}{8}(g^2+g'^2)\,\left(|H_1|^2 - |H_2|^2\right)^2 + \frac{1}{2}\,g^2\,|H_1^\dagger\,H_2|^2\,, \quad (4)$$

where $m_1^2, m_2^2, m_{12}^2$ are soft SUSY-breaking masses and $g, g'$ are the $SU(2)_L \times U(1)_Y$ gauge coupling constants.

[1] In the MSSM there are several additional, more exotic, 2-body decays of the top quark and also a host of 3-body final states worth studying, see [13]. Our SUSY notation is as in this reference

After spontaneous symmetry breaking (SSB), the physical content of the Higgs sector of the MSSM consists of one CP-odd ("pseudoscalar") neutral Higgs, $A^0$, two CP-even neutral Higgs bosons, $h^0, H^0$, and a charged Higgs boson, $H^\pm$. Upon due account of the physical gauge sector, the masses of the various spinless bosons are determined in terms of just three parameters, which can be chosen to be the two vacuum expectation values (VEV's) $< H_2^0 >= v_2$, $< H_1^0 >= v_1$, giving masses to the top and bottom quarks respectively, and one physical Higgs mass. However, due to the SSB constraint

$$v^2 \equiv v_1^2 + v_2^2 = 2M_W^2/g^2 = 2^{-3/2} G_F^{-1} \simeq (174\, GeV)^2\,, \quad (5)$$

where $G_F$ is Fermi's constant in $\mu$-decay, in the end only two parameters suffice to completely specify the MSSM Higgs masses at the tree-level. Moreover, since we are interested in the decay process $t \to H^+ b$, it is natural to take $M_{H^\pm}$ as the physical input mass rather than $M_{A^0}$. As the second independent parameter, one can take the ratio of the two VEV's: $\tan\beta = v_2/v_1$. Then, in lowest order, we have the relations [14]

$$\begin{aligned} M_{A^0}^2 &= M_{H^\pm}^2 - M_W^2\,, \\ M_{H^0,h^0}^2 &= \frac{1}{2}\Big( M_{A^0}^2 + M_Z^2 \\ &\quad \pm \sqrt{(M_{A^0}^2 + M_Z^2)^2 - 4 M_Z^2 M_{A^0}^2 \cos^2 2\beta}\Big)\,, \end{aligned} \quad (6)$$

where $M_{h^0} < M_{H^0}$. It is well-known that these formulas become modified at one-loop [15]. In our case, once $M_{H^\pm}$ is fixed, the other Higgs masses enter the decay rate of $t \to H^+ b$ only through virtual corrections. Notice that if we take $M_{A^0}$ as an input, then the approximate LEP bound $M_{A^0} > 60\, GeV$ [16] on the CP-odd state translates into the lower limit $M_{H^\pm} > 100\, GeV$ which is not significantly modified by the radiative corrections [15].

The charged Higgs can be, as noted above, very sensitive to bottom-quark interactions. Specifically, after expressing the two-doublet Higgs fields of the MSSM in terms of the corresponding mass-eigenstates, the interaction Lagrangian describing the $t\,b\,H^+$-vertex reads as follows [14]:

$$\mathcal{L}_{Hbt} = \frac{g\, V_{tb}}{\sqrt{2} M_W}\, H^-\, \bar{b}\, [m_t \cot\beta\, P_R + m_b \tan\beta\, P_L]\, t + \text{h.c.}\,, \quad (7)$$

where $V_{tb}$ is the corresponding Cabibbo-Kobayashi-Maskawa matrix element, and $P_{L,R} = (1/2)(1 \mp \gamma_5)$ are the projection operators on LH and RH fermions.

In the "$\alpha$-parametrization", where the input parameters are $(\alpha, M_W, M_Z, M_H, m_f, ...)$, the coupling $g$ on (7) stands for $e/s_W$, where $\alpha \equiv \alpha_{\text{e.m.}}(q^2 = 0) = e^2/4\pi$ and $s_W^2 \equiv 1 - c_W^2 \equiv 1 - M_W^2/M_Z^2$. An alternative framework ("$G_F$-parametrization") based on the set of inputs $(G_F, M_W, M_Z, M_H, m_f, ...)$ is also useful, especially at higher orders in perturbation theory (Cf. Sect. 3). At the tree-level, the relation between the two parametrizations is trivial:

$$\frac{G_F}{\sqrt{2}} = \frac{\pi\alpha}{2 M_W^2 s_W^2}\,. \quad (8)$$

From the Lagrangian (7), the tree-level width of the unconventional top quark decay into a charged Higgs boson in the $G_F$-parametrization reads:

$$\begin{aligned} \Gamma^{(0)}(t \to H^+ b) &= \left(\frac{G_F}{8\pi\sqrt{2}}\right) \frac{|V_{tb}|^2}{m_t}\; \lambda^{1/2}(1, \frac{m_b^2}{m_t^2}, \frac{M_{H^\pm}^2}{m_t^2}) \\ &\quad \times [(m_t^2 + m_b^2 - M_{H^\pm}^2)(m_t^2 \cot^2\beta \\ &\quad + m_b^2 \tan^2\beta) + 4 m_t^2 m_b^2]\,, \end{aligned} \quad (9)$$

where

$$\lambda^{1/2}(1, x^2, y^2) \equiv \sqrt{[1 - (x+y)^2][1 - (x-y)^2]}\,. \quad (10)$$

It is useful to compare (9) with the tree-level width of the canonical top quark decay in the SM:

$$\begin{aligned} \Gamma^{(0)}(t \to W^+ b) &= \left(\frac{G_F}{8\pi\sqrt{2}}\right) \frac{|V_{tb}|^2}{m_t}\; \lambda^{1/2}(1, \frac{m_b^2}{m_t^2}, \frac{M_W^2}{m_t^2}) \\ &\quad \times [M_W^2(m_t^2 + m_b^2) \\ &\quad + (m_t^2 - m_b^2)^2 - 2 M_W^4]\,. \end{aligned} \quad (11)$$

The ratio between the two partial widths becomes more transparent upon neglecting the kinematical bottom mass contributions, while retaining all the Yukawa coupling effects:

$$\frac{\Gamma^{(0)}(t \to H^+ b)}{\Gamma^{(0)}(t \to W^+ b)} = \frac{\left(1 - \frac{M_{H^+}^2}{m_t^2}\right)^2 \left[\frac{m_b^2}{m_t^2} \tan^2\beta + \cot^2\beta\right]}{\left(1 - \frac{M_W^2}{m_t^2}\right)^2 \left(1 + 2\frac{M_W^2}{m_t^2}\right)}\,. \quad (12)$$

We see from it that if $M_{H^\pm}$ is not much heavier than $M_W$, then there are two regimes, namely a low and a high $\tan\beta$ regime, where the decay rate of the unconventional top quark decay becomes sizeable as compared to the conventional decay. They can be defined approximately as follows: i) Low $\tan\beta$ regime: $\tan\beta < 2$, and ii) High $\tan\beta$ regime: $\tan\beta \geq m_t/m_b \simeq 35$. The critical regime of the decay $t \to H^+ b$ occurs at the intermediate value $\tan\beta = \sqrt{m_t/m_b} \sim 6$, where the partial width has a pronounced dip. Around this value, the canonical decay $t \to W^+ b$ is dominant over the charged Higgs decay; more specifically, for $3 \lesssim \tan\beta \lesssim 15$ the decay rate of the mode $t \to H^+ b$ is basically irrelevant as compared to the standard mode: $BR(t \to H^+ b) < 10\%$. Therefore, a detailed study of the quantum effects within that interval is of no practical interest.

Even though the approximate perturbative regime for $\tan\beta$ extends over the wide range

$$0.5 \lesssim \tan\beta \lesssim 70\,, \quad (13)$$

we shall emphasize the results obtained in the phenomenologically interesting high $\tan\beta$ region (typically $\tan\beta \gtrsim 30$). As for the low $\tan\beta$ range, while $BR(t \to H^+ b)$ can also be sizeable it turns out that the corresponding quantum effects are generally much smaller than in the high $\tan\beta$ case (Cf. Sect. 5).

Experimentally, and despite naive expectations, the non-SM branching ratio $BR(t \to H^+ b)$ is not as severely

constrained as apparently dictated by the existing measurements of the standard branching ratio at the Tevatron. To assess this fact, notice that one usually assumes that the sole source of top quarks in $p\bar{p}$ collisions is the standard Drell-Yan pair production mechanism $q\,\bar{q} \to t\,\bar{t}$. Now, the observed cross-section is equal to the Drell-Yan production cross-section convoluted over the parton distributions times the squared branching ratio. Schematically,

$$\sigma_{\rm obs.} = \int dq\, d\bar{q}\ \sigma(q\,\bar{q} \to t\,\bar{t})\ \times |BR(t \to W^+ b)|^2\,. \quad (14)$$

However, in the framework of the MSSM, we rather expect a generalization of this formula in the following way:

$$\begin{aligned}\sigma_{\rm obs.} = & \int dq\, d\bar{q}\ \sigma(q\,\bar{q} \to t\,\bar{t})\ \times |BR(t \to W^+ b)|^2 \\ & + \int dq\, d\bar{q}\ \sigma(q\,\bar{q} \to \tilde{g}\,\bar{\tilde{g}}) \\ & \times |BR(\tilde{g} \to t\,\bar{\tilde{t}}_1)|^2 \times |BR(t \to W^+ b)|^2 \\ & + \int dq\, d\bar{q}\ \sigma(q\,\bar{q} \to \tilde{b}_a\,\bar{\tilde{b}}_a) \\ & \times |BR(\tilde{b}_a \to t\,\chi_1^-)|^2 \times |BR(t \to W^+ b)|^2 + \ldots\,, \end{aligned} \quad (15)$$

From (15) we see that if there are alternative (non-SM) sources of top quarks subsequently decaying into the SM final state, $W^+ b$, one cannot rigorously place any stringent upper bound on $BR(t \to W^+ b)$ from the present data. The only restriction being an approximate lower bound $BR(t \to W^+ b) \gtrsim 40 - 50\%$ in order to guarantee the purported standard top quark events at the Tevatron [1]. Thus, from these considerations it is not excluded that the non-SM branching ratio of the top quark, $BR(t \to$"new"$)$, could be as big as the SM one, i.e. $\sim 50\%$.

We stress that at present one cannot exclude (15) since the observed $t \to W^+ b$ final state involves missing energy, as it is also the case for the decays comprising supersymmetric particles. A first step to improve this situation would be to compute some of the additional top quark production cross-sections in the MSSM under given hypotheses on the SUSY spectrum. For instance, the inclusion of the $q\,\bar{q} \to \tilde{g}\,\bar{\tilde{g}}$ mechanism followed by the $\tilde{g} \to t\,\bar{\tilde{t}}_1$ decay has been considered in [17], where it was claimed that $BR(t \to \tilde{t}_1\,\chi_1^0) \simeq 50\%$. By the same token, one cannot place any compelling restriction on $BR(t \to H^+ b)$ from the present FNAL data. In particular, if $\tan\beta$ is large and there exists a relatively light chargino with a non-negligible higgsino component, the third mechanism suggested in (15), namely $q\,\bar{q} \to \tilde{b}_a\,\bar{\tilde{b}}_a$ followed by $\tilde{b}_a \to t\,\chi_1^-$, could also be a rather efficient non-SM source of top quarks. Moreover, if $100\,GeV \lesssim M_{H^\pm} \lesssim 150\,GeV$, then a sizeable portion of the top quarks will decay into a charged Higgs.

Furthermore, it is worth mentioning that the decay mode $t \to H^+ b$ has a distinctive signature which could greatly help in its detection, viz. the fact that at large $\tan\beta$ the emergent charged Higgs would seldom decay into a pair of quark jets, but rather into a $\tau$-lepton and associated neutrino. This follows from inspecting the ratio

$$\begin{aligned}\frac{\Gamma(H^+ \to \tau^+\nu_\tau)}{\Gamma(H^+ \to c\bar{s})} &= \frac{1}{3}\left(\frac{m_\tau}{m_c}\right)^2 \frac{\tan^2\beta}{(m_s^2/m_c^2)\tan^2\beta + \cot^2\beta} \\ &\to \frac{1}{3}\left(\frac{m_\tau}{m_s}\right)^2 > 10 \\ &\quad (\text{for } \tan\beta > \sqrt{m_c/m_s} \gtrsim 2)\,, \end{aligned} \quad (16)$$

where we see that the identification of the charged Higgs decay of the top quark could be a matter of measuring a departure from the universality prediction for all lepton channels. In practice, $\tau$-identification is possible at the Tevatron; and the feasibility of tagging the excess of events with one isolated $\tau$-lepton as compared to events with an additional lepton has also been substantiated by studies of the LHC collaborations. The experimental signature for $t\bar{t} \to H^+ H^-\, b\,\bar{b}$ would differ from $t\bar{t} \to W^+ W^-\, b\,\bar{b}$ by an excess of final states with two $\tau$-leptons and two b-quarks and large missing transverse energy. A study in this direction by the CDF collaboration at the Tevatron [18] has been able to exclude a large portion of the $(\tan\beta, M_{H^\pm})$-plane characterized by $\tan\beta \gtrsim 60$ and $M_{H^\pm}$ below a given value which varies with $\tan\beta$. Thus, we will for definiteness optimize our results in the safe, and phenomenologically interesting, high $\tan\beta$ segment

$$30 \leq \tan\beta \leq 60\,. \quad (17)$$

In short, there are good prospects for detecting the decay $t \to H^+ b$, if it is kinematically accessible. Unfortunately, on the sole basis of computing tree-level effects we cannot find out whether the charged Higgs emerging from that decay is supersymmetric or not. Quantum effects, however, can.

## 3 Renormalization of the $t\,b\,H^+$-vertex

Proceeding closely in parallel with our supersymmetric approach to the conventional decay $t \to W^+ b$ [10,11], we shall address the calculation of the one-loop corrections to the partial width of $t \to H^+ b$ in the MSSM within the context of the on-shell renormalization framework [19]. Again we may use both the $\alpha$ or the $G_F$ parametrizations. At one-loop order, we shall call the former the "$\alpha$-scheme" and the latter the "$G_F$-scheme". Beyond lowest order, the relation between the two on-shell schemes is no longer given by (8) but by

$$\frac{G_F}{\sqrt{2}} = \frac{\pi\alpha}{2M_W^2 s_W^2}(1 + \Delta r^{MSSM})\,, \quad (18)$$

where $\Delta r^{MSSM}$ is the prediction of the parameter $\Delta r$ [19] in the MSSM[2].

Let us sketch the renormalization procedure affecting the parameters and fields related to the $t\,b\,H^+$-vertex, whose interaction Lagrangian was given on (7). In general, the renormalized MSSM Lagrangian $\mathcal{L} \to \mathcal{L} + \delta\mathcal{L}$ is

[2] A dedicated study of $\Delta r^{MSSM}$ has been presented in [20]

obtained following a similar pattern as in the SM, i.e. by attaching multiplicative renormalization constants to each free parameter and field: $g_i \to (1+\delta g_i/g_i)g_i, \Phi_i \to Z_{\Phi_i}^{1/2}\Phi_i$. In our case, in the line of [10,11] we shall use minimal field renormalization, i.e. one renormalization constant per gauge symmetry multiplet [19]. Specifically, for the quark fields under consideration, we have

$$\begin{pmatrix} t_L \\ b_L \end{pmatrix} \to Z_L^{1/2} \begin{pmatrix} t_L \\ b_L \end{pmatrix} \to \begin{pmatrix} (Z_L^t)^{1/2} t_L \\ (Z_L^b)^{1/2} b_L \end{pmatrix},$$
$$b_R \to (Z_R^b)^{1/2} b_R\,, \quad t_R \to (Z_R^t)^{1/2} t_R\,. \tag{19}$$

Here $Z_i = 1 + \delta Z_i$ are the doublet ($Z_L$) and singlet ($Z_R^{t,b}$) field renormalization constants for the top and bottom quarks. Although in the minimal field renormalization scheme there is only one fundamental constant, $Z_L$, per matter doublet, it is useful to work with $Z_L^b = Z_L$ and $Z_L^t$, where the latter differs from the former by a *finite* renormalization effect [19]. To fix all these constants one starts from the usual on-shell mass renormalization condition for fermions, $f$, together with the "residue = 1" condition on the renormalized propagator. These are completely standard procedures, and in this way one obtains [3]

$$\frac{\delta m_f}{m_f} = -\left[\frac{\Sigma_L^f(m_f^2) + \Sigma_R^f(m_f^2)}{2} + \Sigma_S^f(m_f^2)\right], \tag{20}$$

and

$$\delta Z_{L,R}^f = \Sigma_{L,R}^f(m_f^2) + m_f^2[\Sigma_L^{f\,\prime}(m_f^2) + \Sigma_R^{f\,\prime}(m_f^2) + 2\Sigma_S^{f\,\prime}(m_f^2)]\,, \tag{21}$$

where we have decomposed the fermion self-energy according to

$$\Sigma^f(p) = \Sigma_L^f(p^2)\ \not{p}\, P_L + \Sigma_R^f(p^2)\ \not{p}\, P_R + m_f\, \Sigma_S^f(p^2)\,, \tag{22}$$

and used the notation $\Sigma'(p) \equiv \partial\Sigma(p)/\partial p^2$.

One also assigns doublet renormalization constants to the two Higgs doublets (3) of the MSSM:

$$\begin{pmatrix} H_1^0 \\ H_1^- \end{pmatrix} \to Z_{H_1}^{1/2} \begin{pmatrix} H_1^0 \\ H_1^- \end{pmatrix}, \qquad \begin{pmatrix} H_2^+ \\ H_2^0 \end{pmatrix} \to Z_{H_2}^{1/2} \begin{pmatrix} H_2^+ \\ H_2^0 \end{pmatrix}. \tag{23}$$

The renormalization of the gauge sector is related to that of the Higgs sector. In particular, we point out the presence in our decay process $t \to H^+ b$ of the (one-loop induced) mixing term $H^\pm - W^\pm$ for the bare fields, which must be renormalized away for the physical fields $H^\pm$ and $W^\pm$. In order to generate the corresponding Lagrangian counterterm we write

$$W_\mu^\pm \to (Z_2^W)^{1/2} W_\mu^\pm \pm i\,\frac{\delta Z_{HW}}{M_W}\,\partial_\mu H^\pm\,. \tag{24}$$

[3] The sign convention for the self-energy functions is as in [10], which is opposite to that in [19]. Moreover, we understand that in all formulas defining counterterms we are taking the real part of the corresponding functions

Therefore, from

$$\mathcal{L}_{Wbt} = \frac{g}{\sqrt{2}}\, W_\mu^-\, \bar{b}\,\gamma^\mu\, P_L\, t + \text{h.c.} \tag{25}$$

we obtain

$$\begin{aligned}\delta\mathcal{L}_{HW} &= -i\,\delta Z_{HW}\frac{g}{\sqrt{2}M_W}\,\partial_\mu H^-\,\bar{b}\,\gamma^\mu\,P_L\,t + \text{h.c.} \\ &\to \delta Z_{HW}\frac{g}{\sqrt{2}M_W}\,H^-\,\left[m_t\,\bar{b}\,P_R\,t - m_b\,\bar{b}\,P_L\,t\right] \\ &\quad + \text{h.c.}\,,\end{aligned} \tag{26}$$

and in this way it adopts the form of the original vertex (7). In the above expression (24), $Z_2^W = 1 + \delta Z_2^W$ is the usual $SU(2)_L$ gauge triplet renormalization constant given by the formula

$$\begin{aligned}\delta Z_2^W &= \left.\frac{\Sigma_\gamma(k^2)}{k^2}\right|_{k^2=0} - 2\frac{c_W}{s_W}\,\frac{\Sigma_{\gamma Z}(0)}{M_Z^2} \\ &\quad + \frac{c_W^2}{s_W^2}\left(\frac{\delta M_Z^2}{M_Z^2} - \frac{\delta M_W^2}{M_W^2}\right),\end{aligned} \tag{27}$$

and

$$\delta M_W^2 = -\Sigma_W(k^2 = M_W^2)\,, \qquad \delta M_Z^2 = -\Sigma_Z(k^2 = M_Z^2)\,, \tag{28}$$

are the gauge boson mass counterterms enforced by the usual on-shell mass renormalization conditions. Furthermore, $\delta Z_{HW}$ on (24)-(26) is a dimensionless constant associated to the wave-function renormalization mixing among the bare $H^\pm$ and $W^\pm$ fields. Its relation with the doublet renormalization constants, $Z_{H_i} = 1 + \delta Z_{H_i}$, is the following :

$$\delta Z_{HW} = \sin\beta\cos\beta\,\left[\frac{1}{2}\,(\delta Z_{H_2} - \delta Z_{H_1}) + \frac{\delta\tan\beta}{\tan\beta}\right], \tag{29}$$

where $\delta\tan\beta$ is a counterterm associated to the renormalization of $\tan\beta$ (see below). In practice, the most straightforward way to compute $\delta Z_{HW}$ is from the unrenormalized mixed self-energy $\Sigma_{HW}(k^2)$:

$$\delta Z_{HW} = \frac{\Sigma_{HW}(M_{H^\pm}^2)}{M_W^2}\,. \tag{30}$$

For the $SU(2)_L$ gauge coupling constant, we have

$$g \to (1 + \frac{\delta g}{g})g\,, \tag{31}$$

where in the $\alpha$-scheme

$$\frac{\delta g^2}{g^2} = \frac{\delta\alpha}{\alpha} - \frac{c_W^2}{s_W^2}\left(\frac{\delta M_Z^2}{M_Z^2} - \frac{\delta M_W^2}{M_W^2}\right). \tag{32}$$

Let us now outline the renormalization of the Higgs sector of the MSSM [15]. Depending on the particular problem at hand, the renormalization procedure may adopt the CP-odd state $A^0$ as the basic field on which to set the mass and wave-function renormalization conditions. In the present

work, however, since the external Higgs particle is charged, we rather take $H^\pm$ as the basic field. Its mass and field renormalization constants are defined by

$$M^2_{H^\pm} \to M^2_{H^\pm} + \delta M^2_{H^\pm}\,, \qquad H^\pm \to Z^{1/2}_{H^\pm} H^\pm\,. \tag{33}$$

The charged Higgs field renormalization constant, $Z_{H^\pm} = 1 + \delta Z_{H^\pm}$, is of course related to the fundamental doublet renormalization constants introduced on (23), as follows:

$$\delta Z_{H^\pm} = \sin^2\beta\,\delta Z_{H_1} + \cos^2\beta\,\delta Z_{H_2}\,. \tag{34}$$

The structure of the renormalized self-energy is

$$\hat{\Sigma}_{H^\pm}(k^2) = \Sigma_{H^\pm}(k^2) + \delta M^2_{H^\pm} - (k^2 - M^2_{H^\pm})\,\delta Z_{H^\pm}\,, \tag{35}$$

where $\Sigma_{H^\pm}(k^2)$ is the corresponding unrenormalized self-energy.

In order to determine the counterterms, we impose the following renormalization conditions:

i) On-shell mass renormalization condition:

$$\hat{\Sigma}_{H^\pm}(M^2_{H^\pm}) = 0\,, \tag{36}$$

ii) "Residue = 1" condition for the renormalized propagator at the pole mass:

$$\left.\frac{\partial \hat{\Sigma}_{H^\pm}(k^2)}{\partial k^2}\right|_{k^2 = M^2_{H^\pm}} \equiv \hat{\Sigma}'_{H^\pm}(M^2_{H^\pm}) = 0\,. \tag{37}$$

From these conditions one derives

$$\begin{aligned} \delta M^2_{H^\pm} &= -\Sigma_{H^\pm}(M^2_{H^\pm})\,, \\ \delta Z_{H^\pm} &= +\Sigma'_{H^\pm}(M^2_{H^\pm})\,. \end{aligned} \tag{38}$$

Consider next the renormalization of the Higgs potential in the MSSM, (4) [15]. After expanding the neutral components $H^0_1$ and $H^0_2$ around their VEV's $v_1$ and $v_2$, the one-point functions of the resulting CP-even fields are required to vanish, i.e. the tadpole counterterms are constrained to exactly cancel the tadpole diagrams, so that the renormalized tadpoles are zero and the quantities $v_{1,2}$ remain as the VEV's of the renormalized Higgs potential. Notwithstanding, at this stage a prescription to renormalize $\tan\beta = v_2/v_1$,

$$\tan\beta \to \tan\beta + \delta\tan\beta\,, \tag{39}$$

is still called for. There are many possible strategies. The ambiguity is related to the fact that this parameter is just a Lagrangian parameter and as such it is not a physical observable. Its value beyond the tree-level is renormalization scheme dependent. (The situation is similar to the definition of the weak mixing angle $\theta_W$, or equivalently of $\sin^2\theta_W$.) However, even within a given scheme, e.g. the on-shell renormalization scheme, there are some ambiguities that must be fixed. For example, we may wish to define $\tan\beta$ in a process-independent ("universal") way as the ratio $v_2/v_1$ between the true VEV's after renormalization of the Higgs potential [15]. In this case a consistent choice (i.e. a choice capable of renormalizing away the tadpole contributions) is to simultaneously shift the VEV's and the mass parameters of the Higgs potential, (4),

$$\begin{aligned} v_i &\to Z^{1/2}_{H_i}(v_i + \delta v_i)\,, \\ m^2_i &\to Z^{\frac{1}{2}}_{H_i}\,(m^2_i + \delta m^2_i)\,, \\ m^2_{12} &\to Z^{\frac{1}{2}}_{H_1}\,Z^{\frac{1}{2}}_{H_2}\,(m^2_{12} + \delta m^2_{12})\,, \end{aligned} \tag{40}$$

$(i = 1, 2)$ in such a way that $\delta v_1/v_1 = \delta v_2/v_2$. This choice generates the following counterterm for $\tan\beta$ in that scheme:

$$\frac{\delta\tan\beta}{\tan\beta} = \frac{1}{2}\,(\delta Z_{H_2} - \delta Z_{H_1})\,. \tag{41}$$

Nevertheless, this procedure looks very formal and one may eventually like to fix the on-shell renormalization condition on $\tan\beta$ in a more physical way, i.e. by relating it to some concrete physical observable, so that it is the measured value of this observable that is taken as an input rather than the VEV's of the Higgs potential. Following this practical attitude, we choose as a physical observable the decay width of the charged Higgs boson into $\tau$-lepton and associated neutrino: $H^+ \to \tau^+\nu_\tau$. As it has been argued in Sect. 2, this should be a good choice, because: i) When $t \to H^+ b$ is allowed, the decay $H^+ \to \tau^+\nu_\tau$ is the dominant decay of $H^\pm$ already for $\tan\beta \gtrsim 2$; and ii) At high $\tan\beta$, the charged Higgs decay of the top quark can have a sizeable branching ratio.

The interaction Lagrangian describing the decay $H^+ \to \tau^+\nu_\tau$ is directly proportional to $\tan\beta$,

$$\mathcal{L}_{H\tau\nu} = \frac{g\,m_\tau\tan\beta}{\sqrt{2}M_W}\,H^-\,\bar{\tau}\,P_L\,\nu_\tau + \text{h.c.}\,, \tag{42}$$

and the relevant decay width is proportional to $\tan^2\beta$. Whether in the $\alpha$-scheme or in the $G_F$-scheme, it reads:

$$\begin{aligned} \Gamma(H^+ \to \tau^+\nu_\tau) &= \frac{\alpha m^2_{\tau^+}\,M_{H^+}}{8M^2_W s^2_W}\,\tan^2\beta \\ &= \frac{G_F m^2_{\tau^+}\,M_{H^+}}{4\pi\sqrt{2}}\,\tan^2\beta\,(1 - \Delta r^{MSSM}), \end{aligned} \tag{43}$$

where we have used the relation (18). By measuring this decay width one obtains a physical definition of $\tan\beta$ which can be used beyond the tree-level.

Insofar as the determination of the counterterm $\delta\tan\beta$ in our scheme, it can be fixed unambiguously from our Lagrangian definition of $\tan\beta$ on (42) and the renormalization procedure described above. It is straightforward to find:

$$\frac{\delta\tan\beta}{\tan\beta} = \frac{\delta v}{v} - \frac{1}{2}\delta Z_{H^\pm} + \cot\beta\,\delta Z_{HW} + \Delta_\tau\,. \tag{44}$$

Notice the appearance of the vacuum counterterm

$$\frac{\delta v}{v} = \frac{1}{2}\frac{\delta v^2}{v^2} = \frac{1}{2}\frac{\delta M^2_W}{M^2_W} - \frac{1}{2}\frac{\delta g^2}{g^2}\,, \tag{45}$$

which is associated to $v^2 = v_1^2 + v_2^2$, and whose structure is fixed from (5). The last term on (44),

$$\Delta_\tau = -\frac{\delta m_\tau}{m_\tau} - \frac{1}{2}\delta Z_L^{\nu_\tau} - \frac{1}{2}\delta Z_R^{\tau} - F_\tau \,, \qquad (46)$$

is the (finite) process-dependent part of the counterterm. Here $\delta m_\tau/m_\tau$, $\delta Z_L^{\nu_\tau}$ and $\delta Z_R^{\tau}$ are obtained from (20) and (21) (with $m_{\nu_\tau} = 0$ ); they represent the contribution from the mass and wave-function renormalization of the $(\nu_\tau, \tau)$-doublet, including the finite renormalization of the neutrino leg. Finally, $F_\tau$ on (46) is the form factor describing the vertex corrections to the amplitude of $H^+ \to \tau^+ \nu_\tau$.

On comparing (41) and (44) we see that the first definition of $\tan\beta$ appears as though it is free from process-dependent contributions. In practice, however, process-dependent terms are inevitable, irrespective of the definition of $\tan\beta$. In fact, the definition of $\tan\beta$ where $\delta v_1/v_1 = \delta v_2/v_2$ will also develop process-dependent contributions, as can be seen by trying to relate the "universal" value of $\tan\beta$ in that scheme with a physical quantity directly read off some physical observable. For instance, if $M_{A^0}$ is heavy enough, one may define $\tan\beta$ as follows:

$$\begin{aligned}\frac{\Gamma(A^0 \to b\,\bar{b})}{\Gamma(A^0 \to t\,\bar{t})} &= \tan^4\beta\,\frac{m_b^2}{m_t^2}\left(1 - \frac{4\,m_t^2}{M_{A^0}^2}\right)^{-1/2} \\ &\times \left[1 + 4\left(\frac{\delta v_2}{v_2} - \frac{\delta v_1}{v_1}\right)\right. \\ &+ 2\left(\frac{\delta m_b}{m_b} + \frac{1}{2}\delta Z_L^b + \frac{1}{2}\delta Z_R^b - \frac{\delta m_t}{m_t}\right. \\ &\left.\left. - \frac{1}{2}\delta Z_L^t - \frac{1}{2}\delta Z_R^t\right) + \delta V\right] \,, \qquad (47)\end{aligned}$$

where we have neglected $m_b^2 \ll M_{A^0}^2$, and $\delta V$ stands for the vertex corrections to the decay processes $A^0 \to b\,\bar{b}$ and $A^0 \to t\,\bar{t}$. Since the sum of the mass and wave-function renormalization terms along with the vertex corrections is UV-finite, one can consistently choose $\delta v_1/v_1 = \delta v_2/v_2$ leading to (41). Hence, deriving $\tan\beta$ from (47) unavoidably incorporates also some process-dependent contributions.

Any definition of $\tan\beta$ is in principle as good as any other; and in spite of the fact that the corrections themselves may show some dependence on the choice of the particular definition, the physical observables should not depend at all on that choice. However, it can be a practical matter what definition to use in a given situation. For example, our definition of $\tan\beta$ given on (44) should be most adequate for $M_{H^\pm} < m_t - m_b$ and large $\tan\beta$, since then $H^+ \to \tau^+\,\nu_\tau$ is the dominant decay of $H^+$, whereas the definition based on (47) requires also a large value of $\tan\beta$ (to avoid an impractical suppression of the $b\,\bar{b}$ mode); moreover, in order to be operative, it also requires a much heavier charged Higgs boson, since $M_{H^\pm} \simeq M_{A^0} > 2\,m_t$ when the decay $A \to t\bar{t}$ is kinematically open in the MSSM. (Use of light quark final states would, of course, be extremely difficult from the practical point of view.)

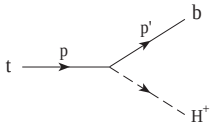


**Fig. 1.** The lowest-order Feynman diagram for the charged Higgs decay of the top quark

Within our context, we use (44) for $\delta\tan\beta/\tan\beta$ in order to compute the one-loop corrections to our decay $t \to H^+ b$. Putting all the pieces together, the counterterm Lagrangian for the vertex $t\,b\,H^+$ follows right away from the bare Lagrangian (7) after re-expressing everything in terms of renormalized parameters and fields in the on-shell scheme. It takes on the form :

$$\begin{aligned}\delta\mathcal{L}_{Hbt} = \frac{g}{\sqrt{2}\,M_W}\,H^-\,\bar{b}\,[&\delta C_R\; m_t\,\cot\beta\;P_R \\ &+\delta C_L\; m_b\,\tan\beta\,P_L]\;t + \text{h.c.}\,, \qquad (48)\end{aligned}$$

with

$$\begin{aligned}\delta C_R &= \frac{\delta m_t}{m_t} - \frac{\delta v}{v} + \frac{1}{2}\,\delta Z_{H^+} + \frac{1}{2}\,\delta Z_L^b + \frac{1}{2}\,\delta Z_R^t \\ &- \frac{\delta\tan\beta}{\tan\beta} + \delta Z_{HW}\;\tan\beta\,, \\ \delta C_L &= \frac{\delta m_b}{m_b} - \frac{\delta v}{v} + \frac{1}{2}\,\delta Z_{H^+} + \frac{1}{2}\,\delta Z_L^t + \frac{1}{2}\,\delta Z_R^b \\ &+ \frac{\delta\tan\beta}{\tan\beta} - \delta Z_{HW}\;\cot\beta\,, \qquad (49)\end{aligned}$$

and where we have set $V_{tb} = 1$ ($V_{tb} = 0.999$ within $\pm 0.1\%$, from unitarity of the CKM-matrix under the assumption of three generations).

## 4 One-loop corrected $\Gamma(t \to H^+ b)$ in the MSSM

As stated in Sect. 2, the study of the decay $t \to H^+ b$ is worthwhile in the small ($\tan\beta < 2$), and most conspicuously in the high ($\tan\beta \geq 30$) $\tan\beta$ region, where the branching ratio can be comparable to the one of the standard decay $t \to W^+ b$. These are, therefore, the regions on which we will focus our search for potentially significant (strong and electroweak like) SUSY quantum corrections to $t \to H^+ b$.

In the following we will describe the relevant electroweak one-loop supersymmetric diagrams entering the amplitude of $t \to H^+ b$ in the MSSM. At the tree-level, the only Feynman diagram is the one in Fig. 1. At the one-loop, we have the diagrams exhibited in Figs. 2–6. The computation of the one-loop diagrams requires to use the full structure of the MSSM Lagrangian[4].

Specifically, Fig. 2 shows the electroweak SUSY vertices involving squarks, charginos and neutralinos. In all

[4] The explicit form of the most relevant pieces of this Lagrangian for our calculation, together with the necessary SUSY notation, is provided in Sect. 3 of [13] and Sect. 2 of [10]

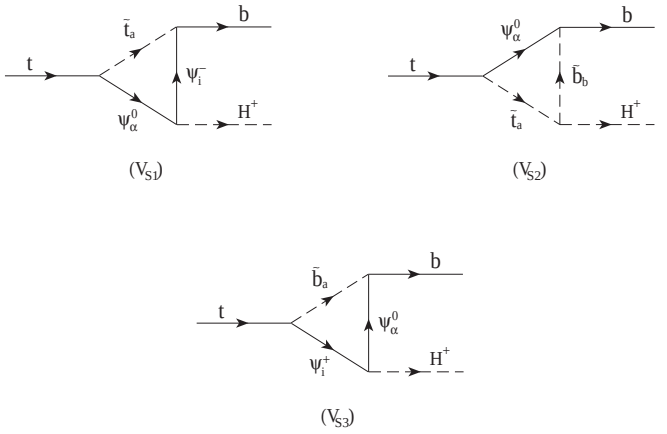


**Fig. 2.** Feynman diagrams, up to one-loop order, for the electroweak SUSY vertex corrections to the decay process $t \to H^+ b$. Each one-loop diagram is summed over all possible values of the mass-eigenstate charginos ($\Psi_i^\pm\,; i = 1, 2$), neutralinos ($\Psi_\alpha^0\,; \alpha = 1, ..., 4$), stop and sbottom squarks ($\tilde{b}_a, \tilde{t}_b\,; a, b = 1, 2$)

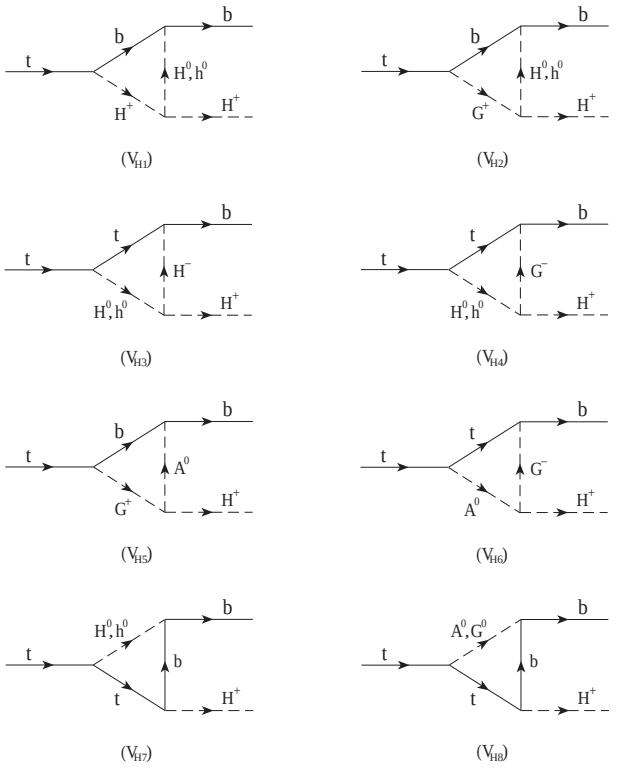


**Fig. 3.** Feynman diagrams, up to one-loop order, for the Higgs and Goldstone boson vertex corrections to the decay process $t \to H^+ b$

these diagrams a sum over all indices is taken for granted. The supersymmetric Higgs particles of the MSSM and Goldstone bosons $G^\pm, G^0$ (in the Feynman gauge) contribute a host of one-loop vertices as well (see Fig. 3). As for the various self-energies, they will be treated as counterterms to the vertices. Their structure is dictated by the Lagrangian (48). Thus, Fig. 4 displays the counterterms $C_{b1} - C_{t4}$ generated from the external bottom and

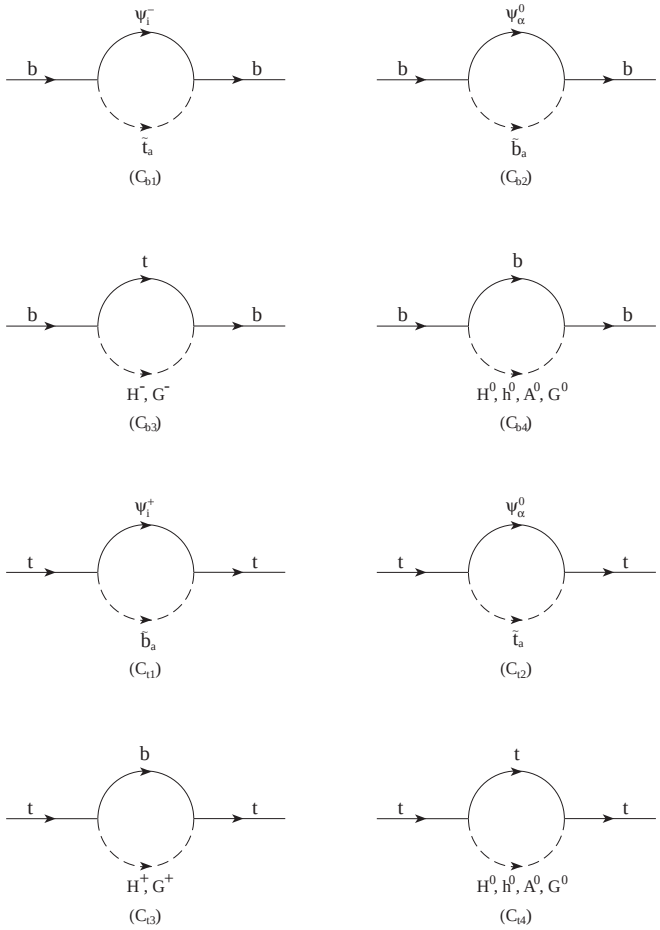


**Fig. 4.** Electroweak self-energy corrections to the top and bottom quark external lines from the various supersymmetric particles, Higgs and Goldstone bosons

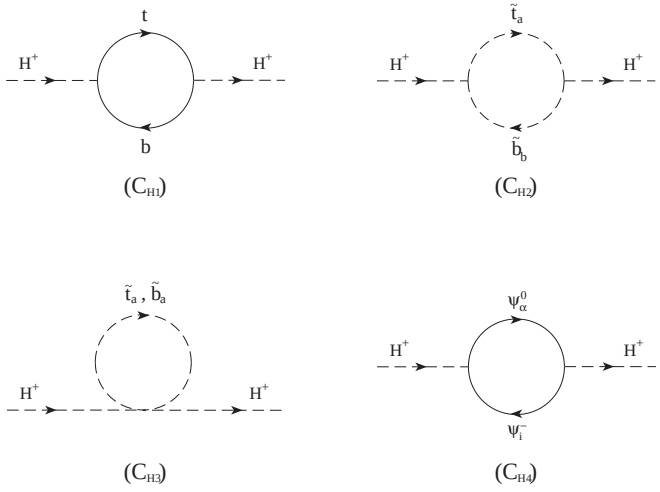


**Fig. 5.** Corrections to the charged Higgs self-energy from the various supersymmetric particles and matter fermions. Only the third quark-squark generation is illustrated

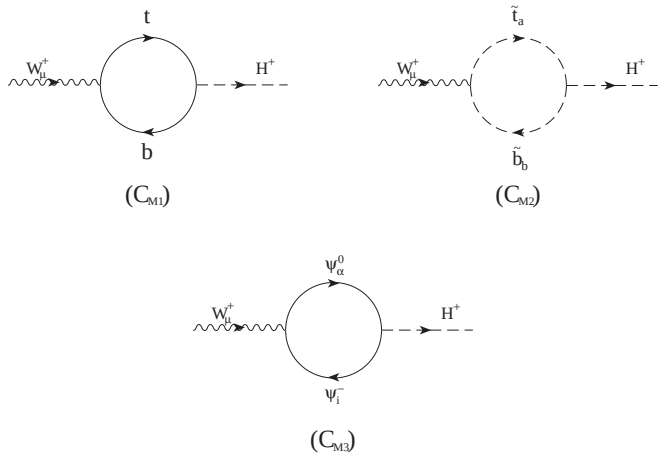


**Fig. 6.** Corrections to the mixed $W^+ - H^+$ self-energy from the various supersymmetric particles and matter fermions. Only the third quark-squark generation is illustrated

top quark lines; they include contributions from supersymmetric particles, Higgs bosons and Goldstone bosons. Similarly, Fig. 5 contains the counterterms $C_{H1} - C_{H4}$ associated to the self-energy of the external charged Higgs boson. A variant of the latter contribution is the mixed $W^+ - H^+$ self-energy counterterms $C_{M1} - C_{M3}$ shown in Fig. 6.

Although we have displayed only the process dependent diagrams, the full analysis should also include the SUSY and Higgs/Goldstone boson contributions to the various universal vacuum polarization effects comprised in our counterterms. However, the calculation of all these pieces has already been discussed in detail long ago in the literature [21] and thus the lengthy formulae accounting for these results will not be explicitly quoted here. Their contribution is not $\tan\beta$-enhanced, but since we wish to compute the full supersymmetric contribution in the relevant regions of the MSSM parameter space, those effects will be included in our numerical code. Finally, the smaller –though numerically overwhelming – subset of strong supersymmetric one-loop graphs are displayed in Fig. 1 of [9]. We will use the formulae from the latter reference in the present analysis to produce the total (electroweak+strong) SUSY correction to our process.

Next let us report on the contributions from the various vertex diagrams and counterterms in the on-shell renormalization scheme. The generic structure of any renormalized vertex function, $\Lambda$, in Figs. 2–3 is composed of two form factors $F_L$, $F_R$ plus the counterterms. Therefore, on making use of the formulae of Sect. 3, one immediately finds:

$$\Lambda = \frac{i\,g}{\sqrt{2}\,M_W}\,\left[m_t\,\cot\beta\,(1+\Lambda_R)\,P_R + m_b\,\tan\beta\,(1+\Lambda_L)\,P_L\right]\,, \tag{50}$$

where

$$\Lambda_R = F_R + \frac{\delta m_t}{m_t} + \frac{1}{2}\,\delta Z_L^b + \frac{1}{2}\,\delta Z_R^t - \Delta_\tau - \frac{\delta v^2}{v^2} + \delta Z_{H^+} + (\tan\beta - \cot\beta)\,\delta Z_{HW}\,,$$
$$\Lambda_L = F_L + \frac{\delta m_b}{m_b} + \frac{1}{2}\,\delta Z_L^t + \frac{1}{2}\,\delta Z_R^b + \Delta_\tau\,. \tag{51}$$

In the following the analytical contributions to the vertex form factors and counterterms will be specified diagram by diagram.

### 4.1 SUSY vertex diagrams

Following the labelling of Feynman graphs in Fig. 2 we write down the terms coming from virtual SUSY particles.

– Diagram $(V_{S1})$: We introduce the shorthands[5]

$$A_\pm \equiv A^{(t)}_{\pm ai} \;\text{ and }\; A^{(0)}_\pm \equiv A^{(t)}_{\pm a\alpha}\,, \tag{52}$$

and define the combinations (omitting indices also for $Q^L_{\alpha i}, Q^R_{\alpha i}$)

$$\begin{aligned} A^{(1)} &= \cos\beta A^*_+ Q^L A^{(0)}_-\,, & E^{(1)} &= \cos\beta A^*_- Q^L A^{(0)}_-\,,\\ B^{(1)} &= \cos\beta A^*_+ Q^L A^{(0)}_+\,, & F^{(1)} &= \cos\beta A^*_- Q^L A^{(0)}_+\,,\\ C^{(1)} &= \sin\beta A^*_+ Q^R A^{(0)}_-\,, & G^{(1)} &= \sin\beta A^*_- Q^R A^{(0)}_-\,,\\ D^{(1)} &= \sin\beta A^*_+ Q^R A^{(0)}_+\,, & H^{(1)} &= \sin\beta A^*_- Q^R A^{(0)}_+\,. \end{aligned} \tag{53}$$

The contribution from diagram $(V_{S1})$ to the form factors $F_L$ and $F_R$ is then

$$\begin{aligned} F_L = M_L\,\Big[&H^{(1)}\tilde{C}_0 + \\ &+m_b\,\left(m_t A^{(1)} + M^0_\alpha B^{(1)} + m_b H^{(1)} + M_i D^{(1)}\right)\\ &\quad\times C_{12}\\ &+m_t\,\left(m_t H^{(1)} + M^0_\alpha G^{(1)} + m_b A^{(1)} + M_i E^{(1)}\right)\\ &\quad\times (C_{11} - C_{12})\\ &+\Big(m_t m_b A^{(1)} + m_t M_i E^{(1)} + M^0_\alpha m_b B^{(1)}\\ &\quad + M_i M^0_\alpha F^{(1)}\Big)\,C_0\Big]\,,\\ F_R = M_R\,\Big[&A^{(1)}\tilde{C}_0 + \\ &+m_b\,\left(m_t H^{(1)} + M^0_\alpha G^{(1)} + m_b A^{(1)} + M_i E^{(1)}\right)\\ &\quad\times C_{12}\\ &+m_t\,\left(m_t A^{(1)} + M^0_\alpha B^{(1)} + m_b H^{(1)} + M_i D^{(1)}\right)\\ &\quad\times (C_{11} - C_{12})\\ &+\Big(m_t m_b H^{(1)} + m_t M_i D^{(1)} + M^0_\alpha m_b G^{(1)}\\ &\quad + M_i M^0_\alpha C^{(1)}\Big)\,C_0\Big]\,, \end{aligned} \tag{54}$$

where the overall coefficients $M_L$ and $M_R$ are the following:

$$M_L = -\frac{ig^2 M_W}{m_b\tan\beta} \qquad M_R = -\frac{ig^2 M_W}{m_t\cot\beta}\,. \tag{55}$$

[5] Again we refer the reader to [13] for notation

The notation for the various 2 and 3-point functions is as in [10]. On (54) they must be evaluated with arguments:

$$C_* = C_* \left(p, p', m_{\tilde{t}_a}, M^0_\alpha, M_i\right) . \tag{56}$$

– Diagram ($V_{S2}$): For this diagram –which in contrast to the others is finite– we introduce the shorthands

$$A^{(b)}_\pm \equiv A^{(b)}_{\pm b\alpha} \;\text{ and }\; A^{(t)}_\pm \equiv A^{(t)}_{\pm a\alpha} , \tag{57}$$

to define the products of coupling matrices

$$\begin{aligned} A^{(2)} &= G_{ba} A^{(b)*}_+ A^{(t)}_- , \quad & C^{(2)} &= G_{ba} A^{(b)*}_- A^{(t)}_- , \\ B^{(2)} &= G_{ba} A^{(b)*}_+ A^{(t)}_+ , \quad & D^{(2)} &= G_{ba} A^{(b)*}_- A^{(t)}_+ . \end{aligned} \tag{58}$$

The contribution to the form factors $F_L$ and $F_R$ from this diagram is

$$\begin{aligned} F_L = -\frac{M_L}{2M_W} \Big[ & m_b B^{(2)} C_{12} + m_t C^{(2)} (C_{11} - C_{12}) \\ & - M^0_\alpha D^{(2)} C_0 \Big] , \\ F_R = -\frac{M_R}{2M_W} \Big[ & m_b C^{(2)} C_{12} + m_t B^{(2)} (C_{11} - C_{12}) \\ & - M^0_\alpha A^{(2)} C_0 \Big] , \end{aligned} \tag{59}$$

the coefficients $M_L$, $M_R$ being those of (55) and the scalar 3-point functions now evaluated with arguments

$$C_* = C_* \left(p, p', M^0_\alpha, m_{\tilde{t}_a}, m_{\tilde{b}_b}\right) . \tag{60}$$

– Diagram ($V_{S3}$): For this diagram we will need

$$A_\pm \equiv A^{(b)}_{\pm ai} \;\text{ and }\; A^{(0)}_\pm \equiv A^{(b)}_{\pm a\alpha} , \tag{61}$$

and again omitting indices we shall use

$$\begin{aligned} A^{(3)} &= \cos\beta A^{(0)*}_+ Q^L A_- , \quad & E^{(3)} &= \cos\beta A^{(0)*}_- Q^L A_- , \\ B^{(3)} &= \cos\beta A^{(0)*}_+ Q^L A_+ , \quad & F^{(3)} &= \cos\beta A^{(0)*}_- Q^L A_+ , \\ C^{(3)} &= \sin\beta A^{(0)*}_+ Q^R A_- , \quad & G^{(3)} &= \sin\beta A^{(0)*}_- Q^R A_- , \\ D^{(3)} &= \sin\beta A^{(0)*}_+ Q^R A_+ , \quad & H^{(3)} &= \sin\beta A^{(0)*}_- Q^R A_+ . \end{aligned} \tag{62}$$

From these definitions the contribution of diagram ($V_{S3}$) to the form factors can be obtained by performing the following changes in that of diagram ($V_{S1}$), (54):

– Everywhere on (54) and (56) replace $M_i \leftrightarrow M^0_\alpha$ and $m_{\tilde{t}_a} \leftrightarrow m_{\tilde{b}_a}$.
– Replace on (54) couplings from (53) with those of (62).
– Include a global minus sign.

### 4.2 Higgs vertex diagrams

Now we consider contributions arising from the exchange of virtual Higgs particles and Goldstone bosons in the Feynman gauge, as shown in Fig. 3. We follow the vertex formula for the form factors by the value of the overall coefficient $N$ and by the arguments of the corresponding 3-point functions.

– Diagram ($V_{H1}$):

$$\begin{aligned} F_L &= N \left[ m_b^2 (C_{12} - C_0) + m_t^2 \cot^2\beta (C_{11} - C_{12}) \right] , \\ F_R &= N m_b^2 [C_{12} - C_0 + \tan^2\beta (C_{11} - C_{12})] , \\ N &= \mp \frac{ig^2}{2} \left( 1 - \frac{\{M^2_{H^0}, M^2_{h^0}\}}{2M_W^2} \right) \\ &\quad \times \frac{\{\cos\alpha, \sin\alpha\}}{\cos\beta} \{\cos(\beta-\alpha), \sin(\beta-\alpha)\} , \\ C_* &= C_* \left(p, p', m_b, M_{H^\pm}, \{M_{H^0}, M_{h^0}\}\right) . \end{aligned}$$

– Diagram ($V_{H2}$):

$$\begin{aligned} F_L &= N \cot\beta [m_t^2 (C_{11} - C_{12}) + m_b^2 (C_0 - C_{12})] , \\ F_R &= N m_b^2 \tan\beta (2C_{12} - C_{11} - C_0) , \\ N &= \frac{ig^2}{4} \frac{\{\cos\alpha, \sin\alpha\}}{\cos\beta} \{\sin(\beta-\alpha), \cos(\beta-\alpha)\} \\ &\quad \times \left( \frac{M^2_{H^\pm}}{M_W^2} - \frac{\{M^2_{H^0}, M^2_{h^0}\}}{M_W^2} \right) , \\ C_* &= C_* \left(p, p', m_b, M_W, \{M_{H^0}, M_{h^0}\}\right) . \end{aligned}$$

– Diagram ($V_{H3}$):

$$\begin{aligned} F_L &= N m_t^2 [\cot^2\beta C_{12} + C_{11} - C_{12} - C_0] , \\ F_R &= N \left[ m_b^2 \tan^2\beta C_{12} + m_t^2 (C_{11} - C_{12} - C_0) \right] , \\ N &= -\frac{ig^2}{2} \frac{\{\sin\alpha, \cos\alpha\}}{\sin\beta} \{\cos(\beta-\alpha), \sin(\beta-\alpha)\} \\ &\quad \times \left( 1 - \frac{\{M^2_{H^0}, M^2_{h^0}\}}{2M_W^2} \right) , \\ C_* &= C_* \left(p, p', m_t, \{M_{H^0}, M_{h^0}\}, M_{H^\pm}\right) . \end{aligned}$$

– Diagram ($V_{H4}$):

$$\begin{aligned} F_L &= N m_t^2 (2C_{12} - C_{11} + C_0) \cot\beta , \\ F_R &= N \left[ -m_b^2 C_{12} + m_t^2 (C_{11} - C_{12} - C_0) \right] \tan\beta , \\ N &= \mp \frac{ig^2}{4} \frac{\{\sin\alpha, \cos\alpha\}}{\sin\beta} \{\sin(\beta-\alpha), \cos(\beta-\alpha)\} \\ &\quad \times \left( \frac{M^2_{H^\pm}}{M_W^2} - \frac{\{M^2_{H^0}, M^2_{h^0}\}}{M_W^2} \right) , \\ C_* &= C_* \left(p, p', m_t, \{M_{H^0}, M_{h^0}\}, M_W\right) . \end{aligned}$$

– Diagram ($V_{H5}$):

$$\begin{aligned} F_L &= N \left[ m_b^2 (C_{12} + C_0) + m_t^2 (C_{11} - C_{12}) \right] , \\ F_R &= N m_b^2 \tan^2\beta (C_{11} + C_0) , \\ N &= -\frac{ig^2}{4} \left( \frac{M^2_{H^\pm}}{M_W^2} - \frac{M^2_{A^0}}{M_W^2} \right) , \\ C_* &= C_* \left(p, p', m_b, M_W, M_{A^0}\right) . \end{aligned}$$

– Diagram ($V_{H6}$):

$$
\begin{aligned}
F_L &= N m_t^2 \cot^2\beta (C_{11} + C_0)\,, \\
F_R &= N\left[m_b^2 C_{12} + m_t^2 (C_{11} - C_{12} + C_0)\right], \\
N &= -\frac{ig^2}{4}\left(\frac{M_{H^\pm}^2}{M_W^2} - \frac{M_{A^0}^2}{M_W^2}\right), \\
C_* &= C_*\left(p, p', m_t, M_{A^0}, M_W\right).
\end{aligned}
$$

– Diagram ($V_{H7}$):

$$
\begin{aligned}
F_L &= N\left[(2m_b^2 C_{11} + \tilde{C}_0 \right. \\
&\quad +2(m_t^2 - m_b^2)(C_{11} - C_{12}))\cot^2\beta \\
&\quad \left. +2m_b^2(C_{11} + 2C_0)\right] m_t^2\,, \\
F_R &= N\left[(2m_b^2 C_{11} + \tilde{C}_0 \right. \\
&\quad +2(m_t^2 - m_b^2)(C_{11} - C_{12}))\tan^2\beta \\
&\quad \left. +2m_t^2(C_{11} + 2C_0)\right] m_b^2\,, \\
N &= \pm\frac{ig^2}{4M_W^2}\frac{\sin\alpha\cos\alpha}{\sin\beta\cos\beta}\,, \\
C_* &= C_*\left(p, p', \{M_{H^0}, M_{h^0}\}, m_t, m_b\right).
\end{aligned}
$$

– Diagram ($V_{H8}$):

$$
\begin{aligned}
F_L &= N m_t^2 \cot^2\beta\, \tilde{C}_0\,, \\
F_R &= N m_b^2 \tan^2\beta\, \tilde{C}_0\,, \\
N &= \mp\frac{ig^2}{4M_W^2}\,, \\
C_* &= C_*\left(p, p', \{M_{A^0}, M_Z\}, m_t, m_b\right).
\end{aligned}
$$

In the equations above, it is understood that the CP-even mixing angle, $\alpha$, is renormalized into $\alpha_{\rm eff}$ by the one-loop Higgs mass relations [15].

As for the SUSY and Higgs contributions to the counterterms, they are much simpler since they just involve 2-point functions. Thus we shall present the full electroweak results by adding up the various sparticle and Higgs effects. In the following formulae, we append labels referring to the specific diagrams on Figs. 4–6.

### 4.3 Counterterms

– Counterterms $\delta m_f\,, \delta Z_L^f\,, \delta Z_R^f$: For a given down-like fermion $b$, and corresponding isospin partner $t$, the fermionic self-energies receive contributions

$$
\begin{aligned}
\Sigma^b_{\{L,R\}}(p^2) &= \Sigma^b_{\{L,R\}}(p^2)\Big|_{(C_{b1})+(C_{b2})} \\
&= -ig^2\left[\left|A^{(t)}_{\pm ai}\right|^2 B_1\left(p, M_i, m_{\tilde{t}_a}\right)\right. \\
&\quad \left. +\frac{1}{2}\left|A^{(b)}_{\pm a\alpha}\right|^2 B_1\left(p, M^0_\alpha, m_{\tilde{b}_a}\right)\right], \\
m_b\Sigma^b_S(p^2) &= m_b\Sigma^b_S(p^2)\big|_{(C_{b1})+(C_{b2})} \\
&= ig^2\left[M_i \mathrm{Re}\left(A^{(t)*}_{+ai}A^{(t)}_{-ai}\right) B_0\left(p, M_i, m_{\tilde{t}_a}\right)\right. \\
&\quad \left. +\frac{1}{2}M^0_\alpha \mathrm{Re}\left(A^{(b)*}_{-a\alpha}A^{(b)}_{+a\alpha}\right)\right. \\
&\quad \left. \times B_0\left(p, M^0_\alpha, m_{\tilde{b}_a}\right)\right], \qquad (63)
\end{aligned}
$$

from SUSY particles, and

$$
\begin{aligned}
\Sigma^b_{\{L,R\}}(p^2) &= \Sigma^b_{\{L,R\}}(p^2)\Big|_{(C_{b3})+(C_{b4})} \\
&= \frac{g^2}{2iM_W^2}\left\{m^2_{\{t,b\}}\right. \\
&\quad \times\left[\{\cot^2\beta, \tan^2\beta\}B_1(p, m_t, M_{H^\pm})\right. \\
&\quad \left. + B_1(p, m_t, M_W)\right] \\
&\quad +\frac{m_b^2}{2\cos^2\beta}\left[\cos^2\alpha\, B_1(p, m_b, M_{H^0})\right. \\
&\quad + \sin^2\alpha\, B_1(p, m_b, M_{h^0}) \\
&\quad + \sin^2\beta\, B_1(p, m_b, M_{A^0}) \\
&\quad \left.\left. + \cos^2\beta\, B_1(p, m_b, M_Z)\right]\right\}, \\
\Sigma^b_S(p^2) &= \Sigma^b_S(p^2)\big|_{(C_{b3})+(C_{b4})} \\
&= -\frac{g^2}{2iM_W^2}\left\{m_t^2\left[B_0(p, m_t, M_{H^\pm})\right.\right. \\
&\quad \left. - B_0(p, m_t, M_W)\right] \\
&\quad +\frac{m_b^2}{2\cos^2\beta}\left[\cos^2\alpha\, B_0(p, m_b, M_{H^0})\right. \\
&\quad + \sin^2\alpha\, B_0(p, m_b, M_{h^0}) \\
&\quad - \sin^2\beta\, B_0(p, m_b, M_{A^0}) \\
&\quad \left.\left. - \cos^2\beta\, B_0(p, m_b, M_Z)\right]\right\}, \qquad (64)
\end{aligned}
$$

from Higgs and Goldstone bosons in the Feynman gauge. To obtain the corresponding expressions for an up-like fermion, $t$, just perform the label substitutions $b \leftrightarrow t$ on (63)-(64); and on (64) replace $\sin\alpha \leftrightarrow \cos\alpha$ and $\sin\beta \leftrightarrow \cos\beta$ (which also implies replacing $\tan\beta \leftrightarrow \cot\beta$).

Introducing the above expressions into (20)-(21) one immediately obtains the SUSY contribution to the counterterms $\delta m_f\,, \delta Z^f_{L,R}$.

– Counterterm $\delta Z_{H^\pm}$:

$$
\begin{aligned}
\delta Z_{H^\pm} &= \delta Z_{H^\pm}|_{(C_{H1})+(C_{H2})+(C_{H3})+(C_{H4})} \\
&= \Sigma'_{H^\pm}(M^2_{H^\pm}) \\
&= -\frac{ig^2 N_C}{M_W^2}\left[(m_b^2\tan^2\beta + m_t^2\cot^2\beta)\right. \\
&\quad \times (B_1 + M^2_{H^\pm}B'_1 + m_b^2 B'_0) \\
&\quad \left. + 2m_b^2 m_t^2 B'_0\right](M_{H^\pm}, m_b, m_t) \\
&\quad + \frac{ig^2}{2M_W^2}N_C\sum_{ab}|G_{ba}|^2 B'_0(M_{H^\pm}, m_{\tilde{b}_b}, m_{\tilde{t}_a}) \\
&\quad - 2ig^2\sum_{i\alpha}\left[\left(\left|Q^L_{\alpha i}\right|^2\cos^2\beta + \left|Q^R_{\alpha i}\right|^2\sin^2\beta\right)\right. \\
&\quad \times (B_1 + M^2_{H^\pm}B'_1 + M^{0\,2}_\alpha B'_0) \\
&\quad \left. + 2M_i M^0_\alpha Re\left(Q^L_{\alpha i}Q^{R*}_{\alpha i}\right)\right. \qquad (65)
\end{aligned}
$$

$$\times \sin\beta\cos\beta B_0'\Big](M_{H^\pm}, M_\alpha^0, M_i)\,.$$

Notice that diagram $(C_{H3})$ gives a vanishing contribution to $\delta Z_{H^\pm}$.

– Counterterm $\delta Z_{HW}$:

$$\begin{aligned}\delta Z_{HW} &= \delta Z_{HW}|_{(C_{M1})+(C_{M2})+(C_{M3})} = \frac{\Sigma_{HW}(M_{H^\pm}^2)}{M_W^2}\\ &= -\frac{ig^2N_C}{M_W^2}\left[m_b^2\tan\beta(B_0+B_1)\right.\\ &\qquad\left.+\,m_t^2\cot\beta B_1\right](M_{H^\pm}, m_b, m_t)\\ &+\frac{ig^2N_C}{2M_W^2}\sum_{ab}G_{ba}R_{1a}^{(t)}R_{1b}^{(b)*}\left[2B_1\right.\\ &\qquad\left.+B_0\right](M_{H^\pm}, m_{\tilde b_b}, m_{\tilde t_a})\\ &+\frac{2ig^2}{M_W}\sum_{i\alpha}\left[M_\alpha^0\left(\cos\beta\, Q_{\alpha i}^{L*}C_{\alpha i}^L\right.\right.\\ &\qquad\left.\left.+\sin\beta\, Q_{\alpha i}^{R*}C_{\alpha i}^R\right)(B_0+B_1)\right.\\ &\quad+M_i\left(\sin\beta\, Q_{\alpha i}^{R*}C_{\alpha i}^L\right.\\ &\quad\left.\left.+\cos\beta\, Q_{\alpha i}^{L*}C_{\alpha i}^R\right)B_1\right](M_{H^\pm}, M_\alpha^0, M_i)\,. \quad (66)\end{aligned}$$

Finally, the evaluation of $\Delta_\tau$ on (46) yields similar bulky analytical formulae, which follow after computing diagrams akin to those in Figs. 2–6 for the MSSM corrections to $H^+ \to \tau^+\nu_\tau$. We refrain from quoting them explicitly here. The numerical effect, though, will be explicitly given in Sect. 5.

We are now ready to furnish the corrected width of $t \to H^+ b$ in the MSSM. It just follows after computing the interference between the tree-level amplitude and the one-loop amplitude. It is convenient to express the result as a relative correction with respect to the tree-level width both in the $\alpha$-scheme and in the $G_F$-scheme. In the former we obtain the relative MSSM correction

$$\begin{aligned}\delta_\alpha^{MSSM} &= \frac{\Gamma - \Gamma_\alpha^{(0)}}{\Gamma_\alpha^{(0)}}\\ &= \frac{N_L}{D}\left[2\,Re(\Lambda_L)\right] + \frac{N_R}{D}\left[2\,Re(\Lambda_R)\right]\\ &+\frac{N_{LR}}{D}\left[2\,Re(\Lambda_L+\Lambda_R)\right], \quad (67)\end{aligned}$$

where the corresponding lowest-order width is

$$\Gamma_\alpha^{(0)} = \left(\frac{\alpha}{s_W^2}\right)\frac{D}{16\,M_W^2\,m_t}\,\lambda^{1/2}(1, \frac{m_b^2}{m_t^2}, \frac{M_{H^\pm}^2}{m_t^2})\,, \quad (68)$$

with

$$\begin{aligned}D &= (m_t^2+m_b^2-M_{H^\pm}^2)\,(m_t^2\cot^2\beta + m_b^2\tan^2\beta)\\ &\quad +4m_t^2m_b^2\,,\\ N_L &= (m_t^2+m_b^2-M_{H^\pm}^2)\,m_b^2\tan^2\beta\,,\\ N_R &= (m_t^2+m_b^2-M_{H^\pm}^2)\,m_t^2\cot^2\beta\,,\\ N_{LR} &= 2m_t^2m_b^2\,. \quad (69)\end{aligned}$$

From these equations it is obvious that at low $\tan\beta$ the relevant quantum effects basically come from the contributions to the form factor $\Lambda_R$ whereas at high $\tan\beta$ they come from $\Lambda_L$.

Using (18) we find that the relative MSSM correction in the $G_F$-parametrization reads

$$\delta_{G_F}^{MSSM} = \frac{\Gamma - \Gamma_{G_F}^{(0)}}{\Gamma_{G_F}^{(0)}} = \delta_\alpha^{MSSM} - \Delta r^{MSSM}\,, \quad (70)$$

where the tree-level width in the $G_F$-scheme, $\Gamma_{G_F}^{(0)}$, is given by (9) and is related to (68) through

$$\Gamma_\alpha^{(0)} = \Gamma_{G_F}^{(0)}\,(1-\Delta r^{MSSM})\,. \quad (71)$$

## 5 Numerical analysis and discussion

Quantum effects should be able to discriminate whether the charged Higgs emerging from the decay $t \to H^+ b$ is supersymmetric or not, for the MSSM provides a well defined prediction of the size of these effects for given values of the sparticle masses. Some work on radiative corrections to the decay width of $t \to H^+ b$ has already appeared in the literature. In particular, the conventional QCD corrections have been evaluated [8] and found to significantly reduce the partial width. The SUSY-QCD corrections are also substantial and the virtual effects mediated by the Higgs bosons have been addressed in different approximations [6]. However, a comprehensive analysis including the genuine SUSY effects themselves has never been attempted. Thus, if only for completeness, we are providing here not only a dedicated treatment of the $R$-odd contributions mediated by the sparticles of the MSSM, but also the fully-fledged pay-off of the supersymmetric Higgs effects.

Before presenting the results of the numerical analysis, it should be clear that the bulk of the high $\tan\beta$ corrections to the decay rate of $t \to H^+ b$ in the MSSM is expected to come from SUSY-QCD. This could already be foreseen from what is known in SUSY GUT models [6]; in fact, in this context a non-vanishing sbottom mixing (which we also assume in our analysis) may lead to important SUSY-QCD quantum effects on the bottom mass, $m_b = m_b^{GUT} + \Delta m_b$, where $\Delta m_b$ is proportional to $M_{LR}^b \to -\mu\tan\beta$ at sufficiently high $\tan\beta$. These are finite threshold effects that one has to include when matching the SM and MSSM renormalization group equations (RGE) at the effective supersymmetric threshold scale, $T_{SUSY}$, above which the RGE evolve according to the MSSM $\beta$-functions in the $\overline{MS}$ scheme [23]. In our case, since the bottom mass is an input parameter for the on-shell scheme, these effects are just fed into the mass counterterm $\delta m_b/m_b$ on (51) and contribute to it with opposite sign ($\delta m_b/m_b = -\Delta m_b/m_b + ...$).

Explicitly, when viewed in terms of diagrams of the electroweak-eigenstate basis, the relevant finite corrections

[6] See [9,22] and references therein


**Fig. 7. a** Leading SUSY-QCD contributions to $\delta m_b/m_b$ in the electroweak-eigenstate basis; **b** Leading supersymmetric Yukawa coupling contributions to $\delta m_b/m_b$ in the electroweak-eigenstate basis

from the bottom mass counterterm are generated by mixed LR-sbottoms and gluino loops (Cf. Fig. 7a):

$$\left(\frac{\delta m_b}{m_b}\right)_{\rm SUSY-QCD} = \frac{2\alpha_s(m_t)}{3\pi}\, m_{\tilde g}\, M^b_{LR}\, I(m_{\tilde b_1}, m_{\tilde b_2}, m_{\tilde g}) \to -\frac{2\alpha_s(m_t)}{3\pi}\, m_{\tilde g}\, \mu \tan\beta\, I(m_{\tilde b_1}, m_{\tilde b_2}, m_{\tilde g})\,, \quad (72)$$

where the last result holds for sufficiently large $\tan\beta$ and for $\mu$ not too small as compared to $A_b$. We have introduced the positive-definite function

$$I(m_1, m_2, m_3) \equiv 16\,\pi^2 i\, C_0(0, 0, m_1, m_2, m_3) = \frac{m_1^2\, m_2^2 \ln\frac{m_1^2}{m_2^2} + m_2^2\, m_3^2 \ln\frac{m_2^2}{m_3^2} + m_1^2\, m_3^2 \ln\frac{m_3^2}{m_1^2}}{(m_1^2 - m_2^2)\,(m_2^2 - m_3^2)\,(m_1^2 - m_3^2)}\,. \quad (73)$$

In addition, we could also foresee potentially large (finite) SUSY electroweak effects from $\delta m_b/m_b$. They are induced by $\tan\beta$-enhanced Yukawa couplings of the type (2). Of course, these effects have already been fully included in the calculation presented in Sect. 3 that we have performed in the mass-eigenstate basis, but it is illustrative of the origin of the leading contributions to pick them up again directly from the diagrams in the electroweak-eigenstate basis. In this case, from loops involving mixed LR-stops and mixed charged higgsinos (Cf. Fig. 7b), one finds:

$$\left(\frac{\delta m_b}{m_b}\right)_{\rm SUSY-Yukawa} = -\frac{h_t\, h_b}{16\pi^2}\,\frac{\mu}{m_b}\, m_t\, M^t_{LR} I(m_{\tilde t_1}, m_{\tilde t_2}, \mu) \to -\frac{h_t^2}{16\pi^2}\,\mu \tan\beta\, A_t\, I(m_{\tilde t_1}, m_{\tilde t_2}, \mu)\,, \quad (74)$$

where again the last expression holds for large enough $\tan\beta$.

Notice that, at variance with (72), the Yukawa coupling correction (74) becomes zero for $A_t = 0$. Although it is true that for nonvanishing $A_t$ and vanishing gluino mass the Yukawa correction could dominate the large $\tan\beta$ effects, we point out that the light gluino scenario is nowadays essentially dead. Recent LEP analyses do exclude light gluinos below $6.3\,GeV$ [24]. Thus, since intermediate gluinos were already ruled out, definitely they must be heavy and most likely of a few hundred $GeV$. Setting $h_t \simeq 1$ at high $\tan\beta$, and assuming that there is no large hierarchy between the sparticle masses, the ratio between (72) and (74) is given, in good approximation, by $4\, m_{\tilde g}/A_t$ times a slowly varying function of the masses of order 1, where the (approximate) proportionality to the gluino mass reflects the very slow decoupling rate of the latter [9]. In view of the Tevatron bounds on the gluino mass [16], and since $A_t$ (as well as $A_b$) cannot increase arbitrarily, we expect that the SUSY-QCD effects will be dominant and even overwhelming for sufficiently heavy gluinos. This conclusion holds good because we have checked that (74) does indeed provide the leading electroweak contribution. However, in contradistinction to the SUSY-QCD case, the total electroweak output is far more complex. There are plenty of additional vertex contributions both from the Higgs sector and from the stop-sbottom/gaugino-higgsino sector where those Yukawa couplings enter once again. Overall, these additional effects turn out to be subleading, and they have been automatically included in our calculation of Sect. 3 within the framework of the mass-eigenstate basis.

We may now pass on to the numerical analysis of the various quantum effects. The results are conveniently cast in terms of the relative correction with respect to the tree-level width:

$$\delta = \frac{\Gamma_H - \Gamma_H^{(0)}}{\Gamma_H^{(0)}} \equiv \frac{\Gamma(t \to H^+ b) - \Gamma^{(0)}(t \to H^+ b)}{\Gamma^{(0)}(t \to H^+ b)}\,. \quad (75)$$

In what follows we understand that $\delta$ defined by (75) is $\delta_\alpha$ – Cf. (67) – i.e. we shall always give our corrections with respect to the tree-level width $\Gamma^0_\alpha$ in the $\alpha$-scheme. The corresponding correction with respect to the tree-level width in the $G_F$-scheme is simply given by (70), where $\Delta r^{MSSM}$ was object of a particular study [20] and therefore it can be easily incorporated, if necessary. Notice, however, that $\Delta r^{MSSM}$ is already tightly bound by the experimental data on $M_Z = 91.1863 \pm 0.0020\,GeV$ at LEP and the ratio $M_W/M_Z$ in $p\bar p$, which lead to $M_W = 80.356 \pm 0.125\,GeV$. Therefore, even without doing the exact theoretical calculation of $\Delta r$ within the MSSM, we already know from

$$\Delta r = 1 - \frac{\pi\alpha}{\sqrt{2}\, G_F}\,\frac{1}{M_W^2\,(1 - M_W^2/M_Z^2)}\,, \quad (76)$$

that $\Delta r^{MSSM}$ must lie in the experimental interval $\Delta r^{\rm exp} \simeq 0.040 \pm 0.018$.

Now, since the corrections computed in Sect. 3 can typically be about one order of magnitude larger than $\Delta r^{\rm MSSM}$, the bulk of the quantum effects on $t \to H^+ b$ is already comprised in the relative correction (75) in the $\alpha$-scheme [7]. Furthermore, in the conditions under study,

[7] For the standard decay $t \to W^+ b$, the situation is quite different since the SM electroweak corrections [25] and the maximal SUSY electroweak corrections [10] in the $\alpha$-scheme are much smaller than for the decay $t \to H^+ b$ , namely they are of the order of $\Delta r$. Therefore, for the standard decay $t \to W^+ b$ there is a significant cancellation between the corrections in the $\alpha$-scheme and $\Delta r$ in most of the $\tan\beta$ range resulting in a substantially diminished correction in the $G_F$-scheme

only a small fraction of $\Delta r^{MSSM}$ is supersymmetric [20], and we should not be dependent on isolating this universal, relatively small, part of the total SUSY correction to $\delta$. To put in a nutshell: if there is to be any hope to measure supersymmetric quantum effects on the charged Higgs decay of the top quark, they should better come from the potentially large, non-oblique, corrections. The SUSY effects contained in $\Delta r^{MSSM}$ [20], instead, will be measured in a much more efficient way from a high precision determination of $M_W$ at LEP 200 and at the Tevatron.

Another useful quantity is the branching ratio

$$B_H \equiv BR(t \to H^+ b) = \frac{\Gamma_H}{\Gamma_W + \Gamma_H + \Gamma_{SUSY}}\,, \qquad (77)$$

where $\Gamma_W \equiv \Gamma(t \to W^+ b)$ and $\Gamma_{SUSY}$ stands for decays of the top quark into SUSY particles. In particular, the potentially important SUSY-QCD mode $t \to \tilde{t}_1\, \tilde{g}$ is kinematically forbidden in most part of our analysis where we usually assume $m_{\tilde{g}} = \mathcal{O}(300)\, GeV$. There may also be the competing electroweak SUSY decays $t \to \tilde{t}_1\, \chi^0_\alpha$ and $t \to \tilde{b}_1\, \chi^+_i$ for some $\alpha = 1, ..., 4$ and some $i = 1, 2$. However, while the former decay is almost always open, it is not $\tan\beta$-enhanced in our favourite segment (17), and the latter decay is phase space obstructed in most of our explored parameter space since we typically assume $m_{\tilde{b}_1} = 150\, GeV$. In general, $\Gamma_{SUSY}$ in (77) is given by

$$\Gamma_{SUSY} = \Gamma(t \to \tilde{t}_1\, \tilde{g}) + \sum_\alpha \Gamma(t \to \tilde{t}_1\, \chi^0_\alpha) + \sum_i \Gamma(t \to \tilde{b}_1\, \chi^+_i)\,. \qquad (78)$$

The various terms contributing to this equation are computed at the tree-level. Similarly, we treat the computation of the partial width of the standard mode $t \to W^+ b$ at the tree-level. This is justified since, as shown in Refs.[10–12], this decay cannot in general develop large supersymmetric radiative corrections, or at least as large as to be comparable to those affecting the charged Higgs mode (for the same value of the input parameters). The reason for it stems from the very different structure of the counterterms for both decays; in particular, the standard decay mode of the top quark does not involve the mass renormalization counterterms for the external fermion lines, and as a consequence the aforementioned large quantum effects associated to the bottom quark self-energy at high $\tan\beta$ are not possible.

Figures 8–13 display in a clear-cut way our main numerical results. We wish to point out that they have been thoroughly checked. Scale independence of $\delta$, (75), and cancellation of UV-divergences have been explicitly verified. Most of the analytical and numerical calculations have been doubled. In particular, we have constructed two independent numerical codes and checked that the two approaches perfectly agree at different stages.

We present our results for $\mu < 0$ [8]. We observe that the leading SUSY-QCD effects on $\delta$ are then positive.

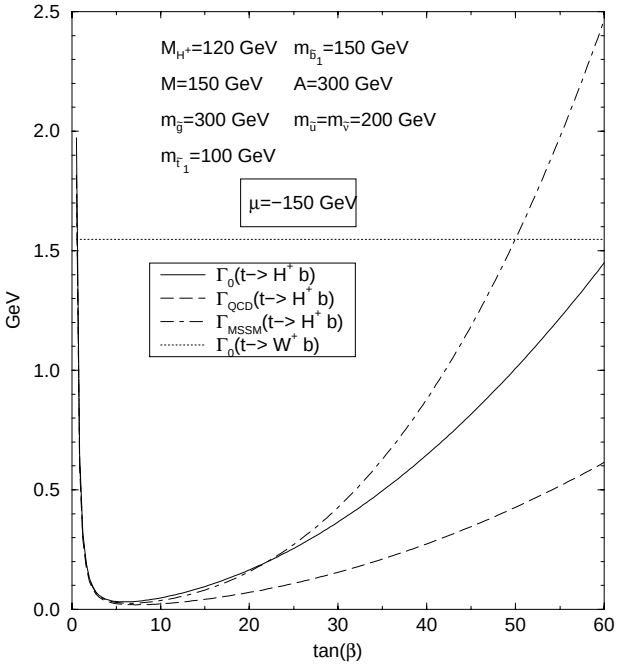


**Fig. 8.** The total partial width, $\Gamma_{MSSM}(t \to H^+ b)$, including all MSSM effects, versus $\tan\beta$, as compared to the tree-level width and the QCD-corrected width. Also plotted is the tree-level partial width of the standard top quark decay, $t \to W^+ b$. The masses of the top and bottom quarks are $m_t = 175\, GeV$ and $m_b = 5\, GeV$, respectively, and the rest of the inputs are explicitly given. We remark that $A_t = A_b = ... \equiv A$ is a common value of the trilinear coupling for all squark and slepton generations. Unless explicitly stated otherwise, the inputs staying at fixed values in the remaining figures are common to the values stated here

This means that in these circumstances the potentially large strong supersymmetric effects are in frank competition with the conventional QCD corrections, which are also very large and stay always negative as will be discussed later on.

Needless to say, a crucial parameter to be investigated is $\tan\beta$. In Fig. 8 we plot the tree-level width, $\Gamma_0(t \to H^+ b)$, and the total partial width, $\Gamma_{MSSM}(t \to H^+ b)$, comprising all the MSSM effects, as a function of $\tan\beta$. Also shown in Fig. 8 is the (tree-level) partial width of the standard top quark decay $t \to W^+ b$, which is (as noted above) far less sensitive to quantum corrections. For convenience, we have included in Fig. 8 a plot of $\Gamma_{\rm QCD}(t \to H^+ b)$, i.e. the partial width that would be obtained in the presence of only the standard QCD corrections. In practice, this is tantamount to saying that $\Gamma_{\rm QCD}(t \to H^+ b)$ is the partial width that would be expected in the absence of SUSY effects, for the electroweak non-supersymmetric

[8] The problem with $\mu > 0$ is that in this case the large SUSY-QCD corrections have the same (negative) sign as the conventional QCD effects, and as a consequence the total MSSM correction can easily blow up above 100%, the branching ratio becoming negative!. To avoid this disaster (from the point of view of perturbation theory!), one must enforce the SUSY-QCD correction to be small enough by assuming sbottom masses of $\mathcal{O}(1)\, TeV$

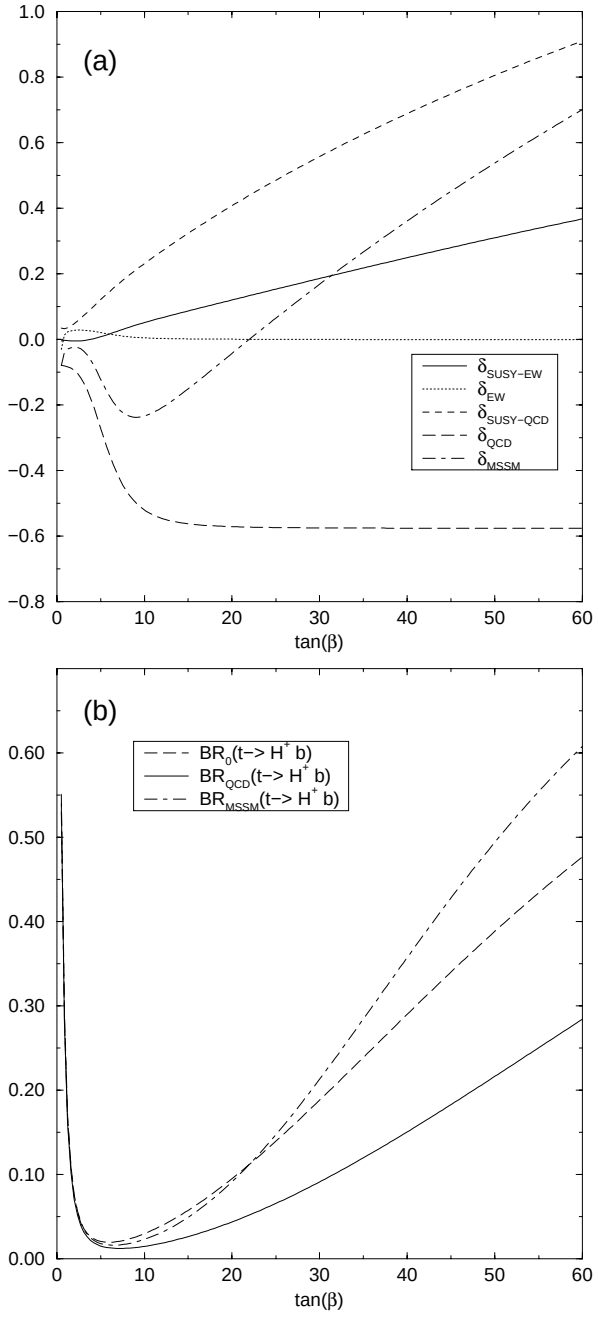


**Fig. 9. a** The relative corrections $\delta$, (75), as a function of $\tan\beta$. Shown are the SUSY-EW, standard EW (i.e. non-supersymmetric electroweak), SUSY-QCD, standard QCD, and total MSSM contribution, (80); **b** The branching ratio (77), as a function of $\tan\beta$; separately shown are the values of this observable after including standard QCD corrections, full MSSM corrections, and the tree-level value

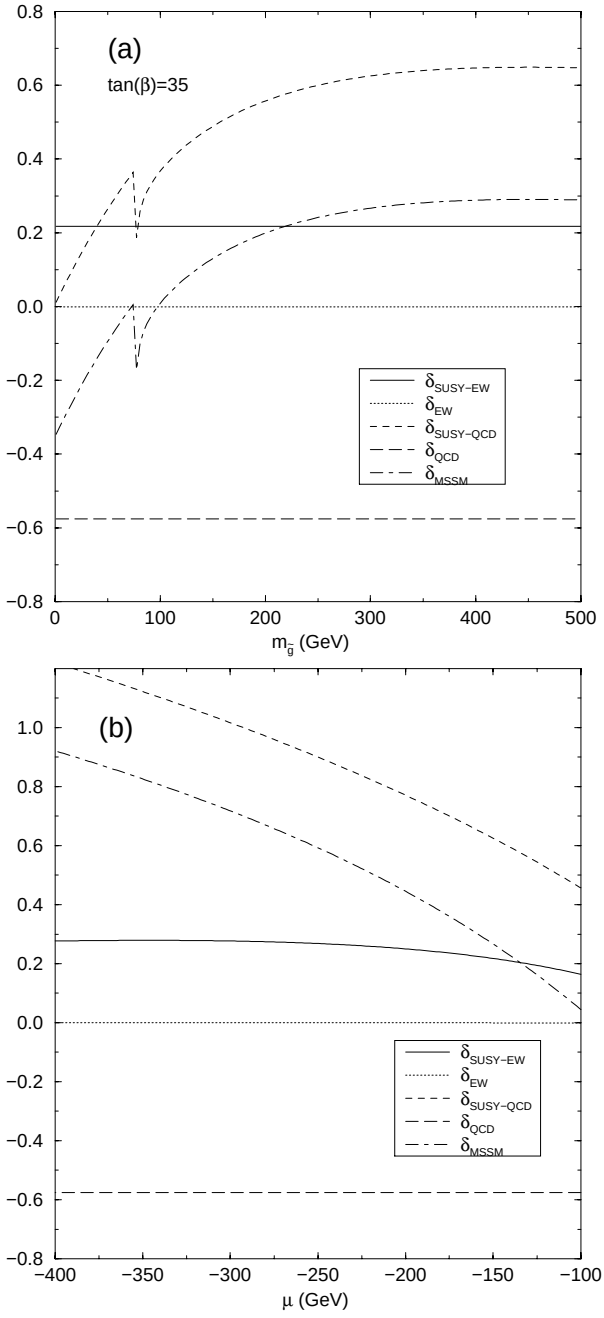


**Fig. 10. a** The relative corrections $\delta$, (75), as a function of the gluino mass, $m_{\tilde{g}}$, for the SUSY-EW, standard EW, SUSY-QCD, standard QCD contributions, and total MSSM contribution, **b** $\delta$ as a function of the supersymmetric Higgs mixing parameter $\mu$ (assuming $\mu < 0$) for the various contributions as in Fig. 9a

corrections turn out to be negligible versus the ordinary QCD effects.

The individual influence of the parameters is tested in Figs. 9 to 13. To appraise the relative importance of the various types of MSSM effects on $\Gamma(t \to H^+ b)$, in Figs. 9a–9b we provide plots for the correction to the partial width, (75), and to the branching ratio, (77), as a function of $\tan\beta$, reflecting the various individual contributions. Specifically, we show in Fig. 9a:

- (i) The supersymmetric electroweak contribution from genuine ($R$-odd) sparticles (denoted $\delta_{\rm SUSY-EW}$), i.e. from sfermions (squarks and sleptons), charginos and neutralinos;
- (ii) The electroweak contribution from non-supersymmetric ($R$-even) particles ($\delta_{EW}$). It is composed of two

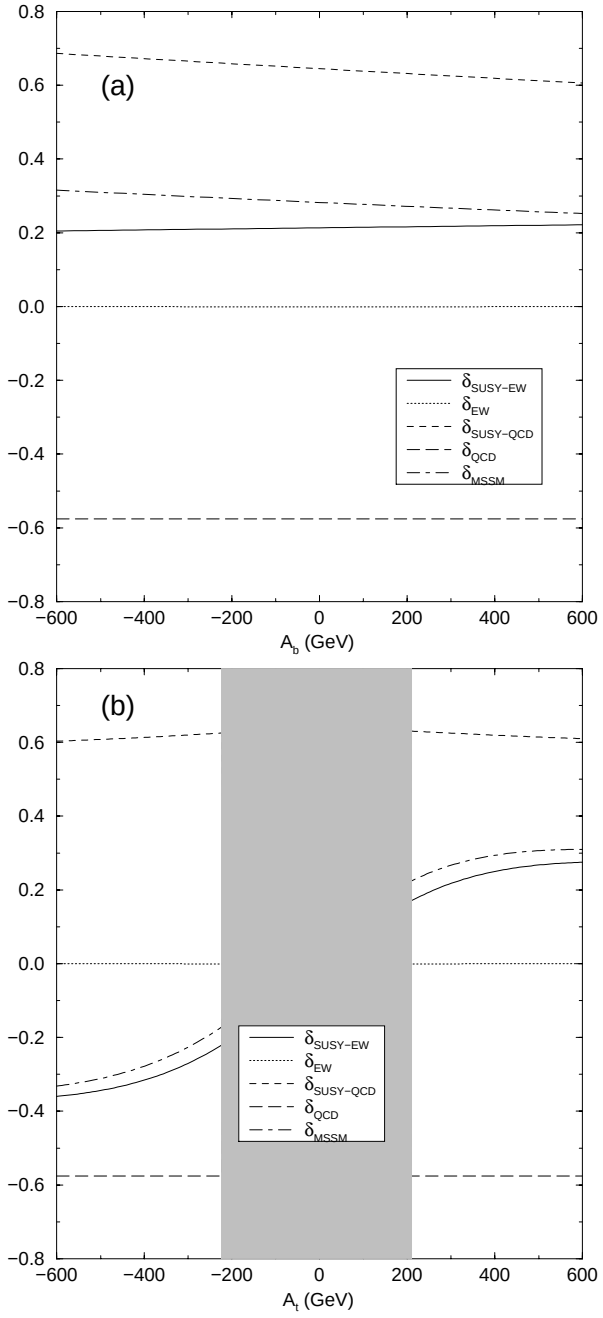


**Fig. 11. a** The relative corrections $\delta$, (75), as a function of the trilinear soft SUSY-breaking parameter $A_b$ in the bottom sector. The other trilinear couplings are kept as in Fig. 8; **b** As in **a**, but for the trilinear soft SUSY-breaking parameter $A_t$ in the top sector. Shown are the same individual and total contributions as in Fig. 9a

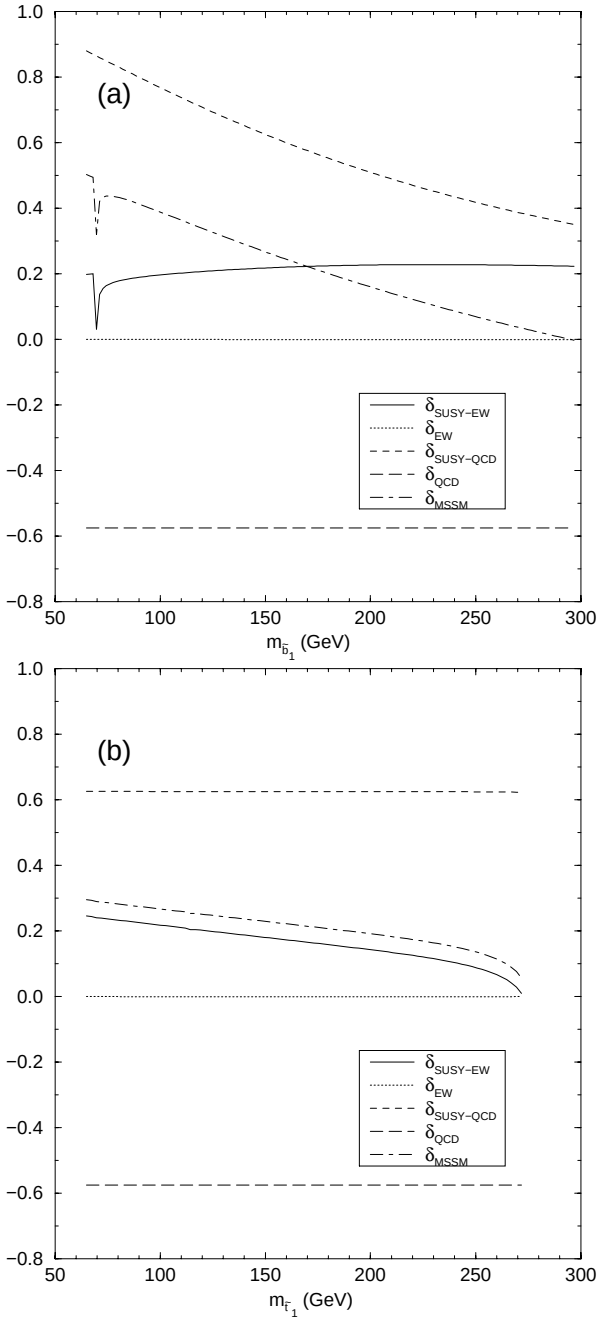


**Fig. 12.** The relative corrections $\delta$, (75), for the various contributions as in Fig. 9a, as a function of: **a** The lightest sbottom mass, $m_{\tilde{b}_1}$; **b** The lightest stop mass, $m_{\tilde{t}_1}$

distinct types of effects, namely, those from Higgs and Goldstone bosons (collectively called "Higgs" contribution, and denoted $\delta_{\rm Higgs}$) plus the leading SM effects [19] from conventional fermions ($\delta_{\rm SM}$):

$$\delta_{EW} = \delta_{\rm Higgs} + \delta_{\rm SM}\,; \tag{79}$$

The remaining non-supersymmetric electroweak effects are subleading and are neglected.

– (iii) The strong supersymmetric contribution (denoted by $\delta_{\rm SUSY-QCD}$) from squarks and gluinos;
– (iv) The strong contribution from conventional quarks and gluons (labelled $\delta_{\rm QCD}$); and
– (v) The total MSSM contribution, $\delta_{\rm MSSM}$, namely, the net sum of all the previous contributions:

$$\delta_{\rm MSSM} = \delta_{\rm SUSY-EW} + \delta_{EW} + \delta_{\rm SUSY-QCD} + \delta_{\rm QCD}. \tag{80}$$

In Fig. 9b we reflect the impact of the MSSM on the branching ratio, as a function of $\tan\beta$; also shown are the

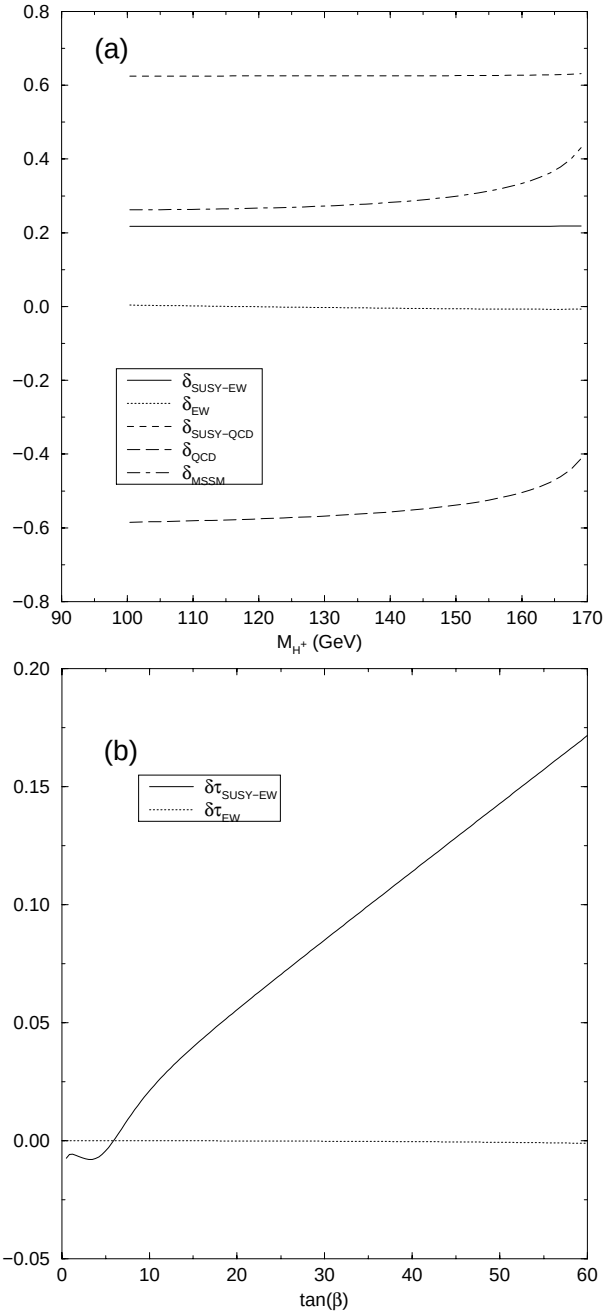


**Fig. 13. a** The relative corrections $\delta$, (75), as a function of the charged Higgs mass; **b** The supersymmetric ($\delta\tau_{\rm SUSY-EW}$) and non-supersymmetric ($\delta\tau_{\rm EW}$) electroweak contributions to $\delta$, (75), from the process-dependent term $\Delta_\tau$, (46), as a function of $\tan\beta$

tree-level value of the branching ratio and the latter quantity after including the (non-supersymmetric) $QCD$ corrections. A typical common set of inputs has been chosen in Figs. 9a–9b such that the supersymmetric electroweak corrections reinforce the strong supersymmetric effects. For this set of inputs, the total MSSM correction to the partial width of $t \to H^+ b$ is positive for $\tan\beta > 20$ (approx.). Remarkably enough, this is so in spite of the huge negative effects induced by conventional QCD. In fact, we see that the gluon yield is overridden by the gluino pay-off provided $\tan\beta$ is sufficiently large: $\tan\beta \geq 30$. Beyond this value, the strength of the supersymmetric loops becomes rapidly overwhelming; e.g. at the representative value $\tan\beta = m_t/m_b = 35$ we find $\delta_{\rm MSSM} \simeq +27\%$; and at $\tan\beta \simeq 50$, which is the preferred value claimed by $SO(10)$ Yukawa coupling unification models [6], the correction is already $\delta_{\rm MSSM} \simeq +55\%$. Quite in contrast, at that $\tan\beta$ one would expect, in the absence of SUSY effects, a (QCD) correction of about $-57\%$, i.e. virtually of the same size but opposite in sign!

Coming back to Fig. 8, we see that, after including the SUSY effects, the partial width of $t \to H^+ b$ equals the partial width of the standard decay $t \to W^+ b$ near the "$SO(10)$" point $\tan\beta = 50$. (The meeting point is actually a bit earlier in $\tan\beta$, after taking into account the known [10,11], negative, SUSY corrections to $t \to W^+ b$, but this effect is not shown in Fig. 8 since it is relatively small.) Now, for the typical set of parameter values introduced in Fig. 8, the top quark decay width into SUSY particles, (78), is rather tiny. Thus it is not surprising that in these conditions the branching ratio of the charged Higgs mode can be remarkably high: $BR(t \to H^+ b) \simeq 50\%$, i.e. basically $50\% - 50\%$ versus the standard decay mode. In contrast, the branching ratio without SUSY effects (i.e. essentially the QCD-corrected branching ratio) is much smaller: at the characteristic $SO(10)$ value, $\tan\beta = 50$, it barely reaches 20%. Clearly, if the SUSY quantum effects are there, they could hardly be missed!

As noted before, even though the dominant MSSM effects are, by far, the QCD and SUSY-QCD ones, they have opposite signs. Therefore, there is a crossover point of the two strongly interacting dynamics, where the conventional QCD loops are fully counterbalanced by the SUSY-QCD loops. This leads to a funny situation, namely, that at the vicinity of that point the total MSSM correction is given by just the subleading, albeit non-negligible, electroweak supersymmetric contribution: $\delta_{\rm MSSM} \simeq \delta_{\rm SUSY-EW}$. The crossover point occurs at $\tan\beta \gtrsim 32 \simeq m_t/m_b$, where $\delta_{\rm SUSY-EW} \gtrsim 20$. For larger and larger $\tan\beta$ beyond $m_t/m_b$, the total (and positive) MSSM correction grows very fast, as we have said, since the SUSY-QCD loops largely overcompensate the standard QCD corrections. As a result, the net effect on the partial width appears to be opposite in sign to what might naively be "expected" (i.e. the QCD sign). Of course, this is not a general result since it depends on the actual values of the MSSM parameters. In the following we wish to explore the various parameter dependences and in particular we want to assess whether a favourable situation as the one just described is likely to happen in an ample portion of the MSSM parameter space. In particular, the value $\tan\beta = m_t/m_b = 35$ will be chosen in all our plots where that parameter must be fixed. We consider it as representative of the low end of the high $\tan\beta$ segment, (17). Thus $\tan\beta = m_t/m_b = 35$ behaves as a sort of threshold point beyond which the MSSM quantum effects on $t \to H^+ b$ take off so fast that they should have indelible experimental consequences on top quark physics.

As regards to the non-supersymmetric electroweak corrections, $\delta_{\rm EW}$, it is apparent from Fig. 9a that they are very small, especially in the high $\tan\beta$ segment. Also in the very low $\tan\beta$ segment, $0.5 \lesssim \tan\beta \lesssim 1$, $\delta_{EW}$ is relatively small. As it happens, we end up with the fact that the complicated Higgs effects result in a tiny contribution, except in the very low $\tan\beta$ end, where e.g. they can reach $-15\%$ at $\tan\beta \simeq 0.5$. In this corner of the parameter space, $\delta_{\rm Higgs}$ becomes the dominant part of $\delta_{\rm MSSM}$ [9].

We come now to briefly discuss the standard QCD effects up to $\mathcal{O}(\alpha_s)$, which involve one-loop gluon corrections and gluon bremsstrahlung [8]. As it is plain from Fig. 9a, $\delta_{\rm QCD}$ is negative-definite and very important in the high $\tan\beta$ segment. It quickly saturates for $\tan\beta \gtrsim 10$ at a large value of order $-60\%$. Therefore, the QCD effects need to be considered in order to isolate the virtual SUSY signature [8]. The leading behaviour of the standard QCD component in the relative correction (75) can be easily assessed by considering the following asymptotic formula

$$\delta_{QCD} = -\frac{2\,\alpha_s}{3\pi(m_b^2\tan^2\beta + m_t^2\cot^2\beta)} \times \left[\frac{4\pi^2-15}{6}(m_b^2\tan^2\beta + m_t^2\cot^2\beta) + 3(4+\tan^2\beta - 2\frac{M_{H^+}^2}{m_t^2}\cot^2\beta)m_b^2\ln\left(\frac{m_t^2}{m_b^2}\right)\right], \quad (81)$$

which we have obtained by expanding the exact one-loop formula up to $\mathcal{O}(m_b^2/m_t^2, M_{H^+}^2/m_t^2)$. Here $\alpha_s \equiv \alpha_s(m_t^2)$, normalized as $\alpha_s(M_Z^2) \simeq 0.12$. The big log factor $\ln(m_t^2/m_b^2)$ originates from the running b-quark mass evaluated at the top quark scale. The correction is seen to be always negative. We point out that while we have used the exact $\mathcal{O}(\alpha_s)$ formula for the numerical evaluation, the approximate expression given above is sufficiently accurate to convey the general features to be expected both at low and at high $\tan\beta$. In particular, for $m_b \neq 0$ and $\tan\beta$ in the relevant high segment (17), the QCD correction becomes very large and saturates at the value

$$\delta_{QCD} = -\frac{2\,\alpha_s}{\pi}\left(\frac{4\pi^2-15}{18} + \ln\frac{m_t^2}{m_b^2}\right) \simeq -59\% \quad (\tan\beta >> \sqrt{m_t/m_b} \simeq 6)\,. \quad (82)$$

At low values of $\tan\beta$, the corrections are much smaller, as it follows from the approximate expression $\delta_{\rm QCD} \simeq (-\alpha_s/\pi)(8\pi^2-30)/18 \simeq -9.5\%$. We remark that for $m_b = 0$ the dependence on $\tan\beta$ totally disappears from (82), so that one would never be able to suspect the large contribution (82) in the high $\tan\beta$ regime. The limit $m_b = 0$, nevertheless, has been considered for the standard QCD corrections in some places of the literature but, as we have seen, it is untenable unless one concentrates on values of $\tan\beta$ of order 1, in which case the relevance of our decay for SUSY is doomed to oblivion. This situation is similar to the one mentioned above concerning the SUSY-QCD corrections in the limit $m_b = 0$, which leads to an scenario totally blind to the outstanding supersymmetric quantum effects obtained for $m_b \neq 0$ at high $\tan\beta$ [9].

Worth noticing is the evolution of the quantities (75) and (77) as a function of the gluino mass (Cf. Fig. 10a). Of course, only the SUSY-QCD component is sensitive to $m_{\tilde g}$. The steep falls in Fig. 10a are associated to the presence of threshold effects occurring at points satisfying $m_{\tilde g} + m_{\tilde t_1} \simeq m_t$. Away from the threshold points, the behaviour of $\delta_{SUSY-QCD}$ is smooth and perfectly consistent with perturbation theory. Of course, the branching ratio (77) is insensitive to these singularities since they are compensated for by the simultaneous opening of the two-body supersymmetric mode $t \to \tilde t_1\,\tilde g$, for $m_{\tilde g} < m_t - m_{\tilde t_1}$. We emphasize that the relevant gluino mass region for the decay $t \to H^+ b$ is not the light gluino region, but the heavy one, the reason being that the important self-energy correction mentioned above, (72), involves a gluino mass insertion. The correction raises with the gluino mass up to a long flat maximum before bending –very gently – into the decoupling regime (far beyond $1\,TeV$). The fact that the decoupling rate of the gluinos appears to be so slow has an obvious phenomenological interest.

Next we consider the sensitivity of our decay on the higgsino-gaugino parameters $(\mu, M)$ characterizing the chargino-neutralino mass matrices. We start with the supersymmetric Higgs mixing mass, $\mu$. As already stated above, we concentrate on the $\mu < 0$ case. We also choose $A_t > 0$, which makes the electroweak corrections to add up with the SUSY-QCD ones. The evolution of the individual contributions (80), together with the total MSSM yield, as a function of $\mu$, is shown in Fig. 10b for given values of the other parameters. We immediately gather from this figure that the total MSSM correction is extremely sensitive to $\mu$. This is already patent at the level of the leading $\delta m_b/m_b$ effects given by (72) and (74). In all figures where a definite $\mu$ is to be chosen, we have taken the moderate value $\mu = -150\,GeV$. As for the sensitivity of the corrections on the $SU(2)_L$-gaugino soft SUSY-breaking parameter, $M$, we have checked that it is virtually non-existent.

There is some slight evolution of the corrections with $A_b$ (Fig. 11a), mainly on the SUSY-QCD side. Once the sign $\mu < 0$ is chosen, the correction is larger for negative values of $A_b$ than for positive values. We have erred on the conservative side by choosing $A_b = +300\,GeV$ wherever this parameter is fixed. As far as $A_t$ is concerned, $\delta_{\rm SUSY-QCD}$ can only evolve as a function of that parameter through vertex corrections, which are proportional to $A_t\cot\beta$; however, at large $\tan\beta$ these are very depressed. The electroweak correction $\delta_{\rm SUSY-EW}$, instead, is very much dependent on $A_t$ (Fig. 11b). We realize that $\delta_{\rm SUSY-EW}$ changes sign with $A_t$ – Cf. the leading piece (74). In Fig. 11b, $\delta_{\rm MSSM}$ also changes sign with $A_t$ just because the parameter set used is such that the conventional QCD effects are almost cancelled by the SUSY-QCD ones. The shaded vertical band in Fig. 11b is excluded by internal consistency in the choice of parameters in Fig. 8.

Another very crucial parameter to be investigated is $m_{\tilde b_1}$. This is because the SUSY-QCD correction hinges a

[9] We have treated in detail the very low $\tan\beta$ segment by including the one-loop renormalization of the Higgs masses [15]

great deal on the value of the sbottom masses, as it is plain from (72). As a matter of fact, a too large a value of $m_{\tilde{b}_1}$ could upside down the leadership of the SUSY-QCD effects. As a typical mass value for all squarks other than the stop we use $m_{\tilde{q}} \geq 150-200\,GeV (\tilde{q} \neq \tilde{t})$. From Fig. 12a we see that provided $m_{\tilde{b}_1} \lesssim 300\,GeV$ the SUSY-QCD effects remain dominant, but they go down the larger is $m_{\tilde{b}_1}$. The electroweak correction $\delta_{SUSY-EW}$, on the other hand, is quite sustained with increasing $m_{\tilde{b}_1}$ and there are parameter configurations where for sufficiently heavy sbottoms the supersymmetric electroweak effects are larger than the SUSY-QCD effects. However, this is not the most likely situation. Obviously, the evolution of the SUSY-QCD corrections with the stop masses is basically flat (Fig. 12b) since the leading contribution is independent of $m_{\tilde{t}_1}$. Therefore, for definiteness we fix $m_{\tilde{t}_1} \simeq 100\,GeV$.

The influence from the sleptons and the other squarks is practically irrelevant as we have verified. They enter the correction through oblique (universal) quantum corrections. The only exception are the $\tau$-sleptons $\tilde{\tau}_a$ ("staus"), since they are involved in the process-dependent (non-oblique) contribution (46), where the $\tau$-lepton Yukawa coupling becomes enhanced at large $\tan\beta$. We have also tested the variation of our results as a function of the charged Higgs mass, $M_{H^+}$, which up to now it has been fixed at $M_{H^+} = 120\,GeV$. We confirm from Fig. 13a that there is nothing special in the chosen value for that parameter since the sensitivity of the correction is generally low.

We close our study of the split corrections by plotting $\delta_\tau$ as a function of $\tan\beta$ (see Fig. 13b). By definition, $\delta_\tau$ is that part of $\delta_{\rm MSSM}$ originating from the full process-dependent term $\Delta_\tau$, (46), which stems from our definition of $\tan\beta$ on (43). This piece of information is relevant enough. In fact, it should be recalled that the quantum corrections described in the previous figures are scheme dependent. In particular, they rely on our definition of $\tan\beta$ given on (43). What is *not* scheme dependent, of course, is the predicted value of the width and branching ratio (Figs. 8 and 9b) after including all the radiative corrections. Now, from Fig. 13b it is clear that the $\Delta_\tau$-term is not negligible, and so there is a process-dependence in our definition of $\tan\beta$, as it was announced in Sect. 3. At first sight, the $\delta_\tau$-effects are not dramatic since they are small as compared to $\delta_{\rm SUSY-QCD}$, but since the latter is cancelled out by standard QCD (for our parameter choice) we end up with $\delta_\tau$ being of the order (roughly half the size) of the electroweak correction $\delta_{\rm SUSY-EW}$.

The main source of process-dependent $\delta_\tau$-effects lies in the corrections generated by the $\tau$-mass counterterm, $\delta m_\tau/m_\tau$, and can be easily picked out in the electroweak-eigenstate basis (see Fig. 14) much in the same way as we did for the $b$-mass counterterm. There are, however, some differences, as can be appraised by comparing the diagrams in Figs. 7 and 14, where we see that in the latter case the effect derives from diagrams involving $\tau$-sleptons with gauginos or mixed gaugino-higgsinos. A straightforward computation of the diagrams (a) + (b) in Fig. 14 yields

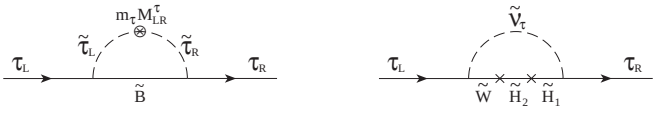


(a) (b)

**Fig. 14.** Leading supersymmetric electroweak contributions to $\delta m_\tau/m_\tau$ in the electroweak-eigenstate basis

$$\frac{\delta m_\tau}{m_\tau} = \frac{g'^2}{16\pi^2}\,\mu\,M'\,\tan\beta\,I(m_{\tilde{\tau}_1}, m_{\tilde{\tau}_2}, M') + \frac{g^2}{16\pi^2}\,\mu\,M\,\tan\beta\,I(\mu, m_{\tilde{\nu}_\tau}, M)\,, \qquad (83)$$

where $g' = g\,s_W/c_W$ and $M', M$ are the soft SUSY-breaking Majorana masses associated to the bino $\tilde{B}$ and winos $\tilde{W}^\pm$, respectively, and the function $I(m_1, m_2, m_3)$ is again given by (73). The sum of the two contributions in (83) indeed shows that it reproduces to within few percent the full numerical result (Cf. Fig. 13b) that we previously obtained in the mass-eigenstate basis, thus confirming that (83) gives the leading contribution.

From all the previous discussion a fact stands out which can be hardly overemphasized, to wit: If the charged Higgs decay mode of the top quark, $t \to H^+ b$, does show up with a branching ratio of order 10% or above (perhaps even as big as 50%), a fairly rich event statistics will be collected at the Tevatron and especially at the LHC. If, in addition, it comes out that the dynamics underlying that decay is truly supersymmetric, then the valuable quantum signatures that our calculation has unveiled over an ample portion of the MSSM parameter space should eventually become manifest and, for sure, we could not miss them.

At present all the collected event statistics on top quarks basically relies on our experimental ability to recognize top quarks from standard patterns (angular distribution, energy spectrum, jet topology etc.) associated to the usual Drell-Yan production mechanism and subsequent SM decays. Notwithstanding, we wish to point out that it should in principle be possible to clutch at the supersymmetric virtual corrections associated to the vertex $t\,b\,H^+$ also through an accurate measurement of the various inclusive top quark and Higgs boson production cross sections in hadron colliders. For instance, in [26] we sketched a few alternative mechanisms which would generate top quark production patterns heavily hinging on the properties of the interaction vertex $t\,b\,H^+$ – and similarly for th $q\,\bar{q}\,A^0(h^0, H^0)$ vertices. Thus, while the vertex $t\,b\,H^+$ could be responsible in part for the decay of the top quark once it is produced, it might as well be at the root of the production process itself at LHC energies, where it could take over from Drell-Yan production.

We conclude our discussion with the following remark. Whereas, on the one hand, one expects that some top quark partial widths will be determined with an accuracy of 10% at the upgraded Tevatron and perhaps better than 10% at LHC [16], on the other hand we believe that from the point of view of an *inclusive* model-independent measurement of the *total* top-quark width, $\Gamma_t$, the future $e^+\,e^-$

supercollider should be a better suited machine [27]. For, in an inclusive measurement, all possible non-SM effects will appear on top of the corresponding SM effects already computed in the literature [25]. Moreover, as shown in [27], one hopes to be able to measure the total top-quark width in $e^+ e^-$ supercolliders at an unmatched precision of $\sim 4\%$ on the basis of a detailed analysis of the threshold effects in the cross-section. Under the assumption that $\Gamma_H \simeq \Gamma_W$, and that the SUSY effects on $\Gamma_t$ are purely virtual effects, it follows that a large SUSY correction of, say 50%, to $t \to H^+ b$ translates into a 20% correction to $\Gamma_t$. This effect could not escape detection. Thus, the combined information from a future $e^+ e^-$ supercollider and from present and medium term hadron machines can be extremely useful to pin down the nature of the observed effects. Our general conclusion is, therefore, extremely encouraging: In view of the potentially large size and large variety of manifestations, quantum effects on top quark and Higgs boson physics could be the clue to the discovery of "virtual" Supersymmetry.

*Acknowledgements.* One of us (JS) is indebted to M. Carena, W. Hollik and C. Wagner for useful conversations. He also thanks the hospitality and financial support provided by the CERN Theory Division where this work was finished. This work has also been partially supported by CICYT under project No. AEN93-0474. The work of DG and JG has been financed by grants of the Comissionat per a Universitats i Recerca, Generalitat de Catalunya.

## References

1. F. Abe et al. (CDF Collab.), Phys. Rev. Lett. **74** (1995) 2626; S. Abachi et al. (D0 Collab.), Phys. Rev. Lett. **74** (1995) 2632
2. P. Grannis, talk at the 28th International Conference on High Energy Physics, Warsaw, Poland, July 25-31th 1996
3. D. Shaile, P.M. Zerwas, Phys. Rev. **D 45** (1992) 3262
4. H. Nilles, Phys. Rep. **110** (1984) 1; H. Haber, G. Kane, Phys. Rep. **117** (1985) 75; A. Lahanas, D. Nanopoulos, Phys. Rep. **145** (1987) 1; See also the exhaustive reprint collection **Supersymmetry** (2 vols.), ed. S. Ferrara (North Holland/World Scientific, Singapore, 1987)
5. W. de Boer, A. Dabelstein, W. Hollik, W. Mösle, U. Schwickkerath, Updated global fits of the SM and the MSSM to electroweak precision data, preprint IEKKA.96-07 [hep-ph/9609209]
6. M. Carena, S. Pokorski, C.E.M. Wagner, Nucl. Phys. **B 426** (1994) 269; L.J. Hall, R. Rattazzi, U. Sarid, Phys. Rev. **D 50** (1994) 7048; R. Rattazzi, U. Sarid, Phys. Rev. **D 53** (1996) 1553
7. I. Bigi, Y. Dokshitzer, V. Khoze, J. Kühn, P. Zerwas, Phys. Lett. **B 181** (1986) 157; V. Barger, R.J.N. Phillips, Phys. Rev. **D 41** (1990) 884; A.C. Bawa, C.S. Kim, A.D. Martin Z. Phys. **C 47** (1990) 95; M. Drees, D.P. Roy, Phys. Lett. **B 269** (1991) 155; B.K. Bullock, K. Hagiwara, A.D. Martin, Phys. Rev. Lett. **67** (1991) 3055; W. Bernreuther et al., in Proc. of the Workshop on $e^+e^-$ Collisions at 500 GeV: The Physics Potential, Hamburg, 1991, ed. P.M. Zerwas; preprint DESY 92–123A (1992); Z. Kunszt, F. Zwirner, Nucl. Phys. **B 385** (1992) 3; D.P. Roy, Phys. Lett. **B 283** (1992) 403
8. A. Czarnecki, S. Davidson, Phys. Rev. **D 48** (1993) 4183; **D 47** (1993) 3063
9. J. Guasch, R.A. Jiménez, J. Solà, Phys. Lett. **B 360** (1995) 47
10. D. Garcia, W. Hollik, R.A. Jiménez, J. Solà, Nucl. Phys. **B 427** (1994) 53
11. A. Dabelstein, W. Hollik, R.A. Jiménez, C. Jünger, J. Solà, Nucl. Phys. **B 456** (1995) 75
12. B. Grzadkowski, W. Hollik, Nucl. Phys. **B 384** (1992) 101; A. Denner, A.H. Hoang, Nucl. Phys. **B 397** (1993) 483
13. J. Guasch, J. Solà, Z. Phys. **C 74** (1997) 337
14. J.F. Gunion, H.E. Haber, G.L. Kane, S. Dawson, The Higgs Hunters' Guide (Addison-Wesley, Menlo-Park, 1990)
15. J. Ellis, G. Ridolfi, F. Zwirner, Phys. Lett. **B 262** (1991) 477; A. Brignole, J. Ellis, G. Ridolfi, F. Zwirner, Phys. Lett. **B 271** (1991) 123; H.E. Haber, R. Hempfling, Phys. Rev. Lett. **66** (1991) 1815; Phys. Rev. **D 48** (1993) 4280; H.E. Haber, in: Perspectives on Higgs Physics, Advanced Series on Directions in High Energy Physics, Vol.13, ed. by G.L. Kane (World Scientific, Singapore, 1993)
16. Talks of E. Gross, G. Chiarelli, A. Kharchilava, J. Thompson, Rencontres de Moriond, Les Arcs, March 1997
17. G.L. Kane, S. Mrenna, Phys. Rev. Lett. **77** (1996) 3502; T. Kon, T. Nonaka, Phys. Rev. **D 50** (1994) 6005
18. J. Conway, talk given at SUSY 96, Univ. of Maryland, College Park, USA, May 29th-June 1st 1996, published in: Nucl. Phys. B (Proc. Suppl.) 52A (1997) p.8 , ed. R. Mohapatra and A. Rasin
19. M. Böhm, H. Spiesberger, W. Hollik, Fortschr. Phys. **34** (1986) 687; W. Hollik, Fortschr. Phys. **38** (1990) 165; W. Hollik, in: Precision Tests of the Standard Electroweak Model, Advanced Series in Directions in High Energy Physics, ed. by P. Langacker (World Scientific, Singapore, 1995)
20. D. Garcia, J. Solà, Mod. Phys. Lett. **A 9** (1994) 211; P.H. Chankowski, A. Dabelstein, W. Hollik, W. Mösle, S. Pokorski, J. Rosiek, Nucl. Phys. **B 417** (1994) 101
21. J. Grifols, J. Solà, Nucl. Phys. **B 253** (1985) 47; Phys. Lett. **B 137** (1984) 257; For a detailed review, see: J. Solà, in: Phenomenological Aspects of Supersymmetry, ed. W. Hollik, R. Rückl and J. Wess (Springer -Verlag, Lecture Notes in Physics **405**, 1992) p. 187
22. C.S. Li, B.Q. Hu, J.M. Yang, Phys. Rev. **D 47** (1993) 2865
23. M. Carena, S. Pokorski, C.E.M. Wagner Nucl. Phys. **B 406** (1993) 59
24. The ALEPH Collab., preprint CERN-PPE/97-002 (January, 1997)
25. M. Jezabek, J.H. Kühn, Nucl. Phys. **B 314** (1989) 1; *ibid* **B 320** (1989) 20; C.S. Li, R.J. Oakes, T.C. Yuan, Phys. Rev. **D 43** (1991) 3759; G. Eilam, R.R. Mendel, R. Migneron, A. Soni, Phys. Rev. Lett. **66** (1991) 3105; A. Denner, T. Sack, Z. Phys. **C 46** (1990) 653; Nucl. Phys. **B 358** (1991) 46; B.A. Irwin, B. Magnolis, H.D. Trottier, Phys. Lett. **B 256** (1991) 533; T.C. Yuan, C.-P. Yuan, Phys. Rev. **D 44** (1991) 3603
26. R.A. Jiménez, J. Solà, Phys. Lett. **B 389** (1996) 53; J.A. Coarasa, R.A. Jiménez, J. Solà, Phys. Lett. **B 389** (1996) 312
27. K. Fujii, T. Matsui, Phys. Rev. **50** (1994) 4341.